SPRINGER BRIEFS IN APPLIED SCIENCES AND TECHNOLOGY · COMPUTATIONAL INTELLIGENCE

Rodrick Wallace

# Canonical Instabilities of Autonomous Vehicle Systems

## The Unsettling Reality Behind the Dreams of Greed

Springer

# SpringerBriefs in Applied Sciences and Technology

## Computational Intelligence

**Series editor**

Janusz Kacprzyk, Polish Academy of Sciences, Systems Research Institute, Warsaw, Poland

The series “Studies in Computational Intelligence” (SCI) publishes new developments and advances in the various areas of computational intelligence—quickly and with a high quality. The intent is to cover the theory, applications, and design methods of computational intelligence, as embedded in the fields of engineering, computer science, physics and life sciences, as well as the methodologies behind them. The series contains monographs, lecture notes and edited volumes in computational intelligence spanning the areas of neural networks, connectionist systems, genetic algorithms, evolutionary computation, artificial intelligence, cellular automata, self-organizing systems, soft computing, fuzzy systems, and hybrid intelligent systems. Of particular value to both the contributors and the readership are the short publication timeframe and the world-wide distribution, which enable both wide and rapid dissemination of research output.

More information about this series at http://www.springer.com/series/10618

Rodrick Wallace

# Canonical Instabilities of Autonomous Vehicle Systems

## The Unsettling Reality Behind the Dreams of Greed

Springer

Rodrick Wallace
New York State Psychiatric Institute
Columbia University
New York, NY
USA

ISSN 2191-530X ISSN 2191-5318 (electronic)
SpringerBriefs in Applied Sciences and Technology
ISSN 2520-8551 ISSN 2520-856X (electronic)
SpringerBriefs in Computational Intelligence
ISBN 978-3-319-69934-9 ISBN 978-3-319-69935-6 (eBook)
https://doi.org/10.1007/978-3-319-69935-6

Library of Congress Control Number: 2017956751



Printed on acid-free paper

This Springer imprint is published by Springer Nature
The registered company is Springer International Publishing AG
The registered company address is: Gewerbestrasse 11, 6330 Cham, Switzerland

# Preface

> *...[T]he psychological actions of drivers make traffic different from any other flow* (Orosz et al. 2010).

The asymptotic limit theorems of control and information theories make it possible to explore the dynamics of collapse likely to afflict systems of autonomous ground vehicles that communicate with each other and with an embedding intelligent roadway. A vehicle/road system is inherently unstable in the control theory sense as a consequence of the basic irregularities of the traffic stream, the road network, and their interactions, placing it in the realm of the data rate theorem that mandates a minimum necessary rate of control information for stability. It appears that such V2V/V2I systems will experience large-scale failures analogous to the vast propagating fronts of power network blackouts, and possibly less benign, but more subtle patterns of individual, platoon, and mesoscale dysfunction.

An atomistic perspective on autonomous ground vehicles—seeing them as having only local dynamics in an embedding traffic stream—embodies a profound failure of insight. Traffic light strategies, road quality, the inevitably rapid-shifting "road map space", the dynamic composition of the traffic stream, communication and machine sensory system bandwidth limits, and so on, create the synergistic context in which single vehicles operate. It is necessary to understand the dynamics of that full system, not simply the behavior of an individual vehicle atom within it. The properties of that system will be both overtly and subtly emergent—subject to sudden "phase transitions" into both massively and locally unstable modes—as will the responses of individual cognitive vehicles enmeshed in context, whether controlled by humans or computers. The triggering of adverse events at various scales and levels of organization by unfriendly external agents will likely become routine.

In sum, while clever V2V/V2I management strategies might keep traffic streams temporarily in a "supercooled" high-flow mode beyond well-understood critical vehicle densities, such a state is notoriously unstable, subject to both random and deliberately caused "condensation" into large-scale frozen zones. More subtle

patterns of individual vehicle and mesoscale "psychopathology" characterizing autonomous systems may be even less benign (Wallace 2017).

Despite marketing hype and other forms of wishful thinking, the safe operation of large-scale V2V/V2I autonomous vehicle systems may be exceedingly arduous at best, and, at worst, simply not possible, particularly in the US context of rapid social and infrastructure deterioration.

It has been said that "The language of business is the language of dreams". Business dreams, as we are now seeing, do not serve as a sound foundation for the design and implementation of public policies affecting the well-being of large populations.

New York, USA Rodrick Wallace

# Contents


**1 Central Problems** . . . . . 1

**2 Dynamics of Service Collapse** . . . . . 7
- 2.1 Introduction . . . . . 7
- 2.2 Multimodal Traffic on Bad Roads . . . . . 9
- 2.3 The Dynamic Model . . . . . 10
- 2.4 Multiple Phases of Dysfunction . . . . . 13

**3 The 'Macroscopic Fundamental Diagram'** . . . . . 17
- 3.1 Introduction . . . . . 17
- 3.2 Intractability of the MFD . . . . . 21
- 3.3 Hysteresis Lock-In of a Pathological Mode . . . . . 29
- 3.4 Groupoid Synergism Redux . . . . . 30

**4 Conclusions** . . . . . 31

**5 Mathematical Appendix** . . . . . 35
- 5.1 An RDT Approach to the DRT . . . . . 35
- 5.2 A Black-Scholes Model . . . . . 37
- 5.3 Groupoids . . . . . 38
- 5.4 Morse Theory . . . . . 40

**6 References** . . . . . 43

# About the Author

**Rodrick Wallace** received an undergraduate degree in mathematics and a Ph.D. in physics from Columbia University. He completed postdoctoral training in the epidemiology of mental disorders at Rutgers University and is a research scientist in the Division of Epidemiology of the New York State Psychiatric Institute. A past recipient of an Investigator Award in Health Policy Research from the Robert Wood Johnson Foundation, he was technical director of a public interest consulting firm for a decade before returning to research and is the author of numerous peer-reviewed papers and books across a variety of disciplines. His work focuses on how government policy and socioeconomic structure determine patterns of public health and public order. This monograph is, in fact, an expansion of a chapter from his recent book *Computational Psychiatry: A systems biology approach to the epigenetics of mental disorders*, Springer, New York (2017), which uses similar methods to examine the failure of cognition at and across different modalities, scales, and levels of organization.

# Chapter 1
# Central Problems

Current marketing hype surrounding autonomous vehicles runs something like this:

> Since more than 90% of highway deaths are related to driver error, automating out the driver will reduce loss of life by more than 90%.

Individual vehicles, however, are nested and enmeshed within larger milieus, creating a multi-scale, multi-level synergism determining crash and fatality rates. Individual vehicles are only one part of that system, not the system itself. Asserting that part of a thing is the whole thing is the infamous *mereological fallacy*, an important tool for the construction of political lies and other forms of advertising.

One is reminded of another—if different—logical fallacy:

> If a woman can gestate a child in nine months, nine women should be able to do it in a month.

Given the inherently complicated nature of transport system safety, assertions regarding the effects of autonomous vehicles on traffic fatalities are entirely speculative and cannot be used as a sound basis for policy development.

Here, we ask a more fundamental question: are large-scale autonomous vehicle systems actually practical, particularly in the context of a rapidly deteriorating social and physical infrastructure? To do this, we examine an 'end stage' limit in which many different kinds of vehicles communicate with each other (V2V), and with an intelligent roadway infrastructure (V2I), both embedded in a highly stochastic environment.

In effect, we use a variety of mathematical models to explore the dynamics of a rapid-acting, inherently unstable command, communication and control system ($C^3$) that is cognitive in the sense that it must, in an appropriate 'real time', evaluate a large number possible actions and choose a small subset for implementation. Such choice decreases uncertainty, in a formal manner, and reduction in uncertainty implies the existence of an information source (Wallace 2012, 2015a).

We particularly study autonomous V2V/V2I systems through the prism of the Data Rate Theorem (Nair et al. 2007), extending the argument to more general phase



R. Wallace, *Canonical Instabilities of Autonomous Vehicle Systems*,
SpringerBriefs in Computational Intelligence,
https://doi.org/10.1007/978-3-319-69935-6_1

transition analogs, and developing statistical tools useful at different scales and levels of organization.

As Box and Draper (1987) put it, 'all mathematical models are wrong, but some are useful'. Here, we necessarily employ a variety of mathematical tools to explore alternate perspectives on complex dynamic structures that are cognitive at micro, meso, and macro scales and levels of organization. In a more limited way, even physical phenomena require different models at different scales—quantum mechanics for atoms, classical mechanics for bridges. The understanding, control, and remediation of multi-scale cognitive phenomena in biology, the social sciences, or institutional ecology simply cannot be done using some analog to Maxwell's equations for electrodynamics or Einstein's equations for gravity, and large autonomous vehicle systems fall under similar constraint. This is particularly so in view of the essential unsolved—and perhaps conventionally unsolvable—nature of the underlying traffic and hydrodynamic flow conundrums (Birkoff 1960; Ruelle 1983).

V2V/V2I autonomous systems operate along geodesics in a densely convoluted 'map quotient space' that is in contrast to the much more straightforward problem of air traffic control, where locally stable vehicle paths are seen as thick braid geodesics in a simpler Euclidean quotient space (Hu et al. 2001). Such geodesics are generalizations of the streamline characteristics of hydrodynamic flow (Landau and Lifshitz 1987).

Hu et al. (2001) show that, in the context of air traffic control, finding collision-free maneuvers for multiple agents on a Euclidean plane surface $\mathscr{R}^2$ is the same as finding the shortest geodesic in a particular manifold with nonsmooth boundary. Given $n$ vehicles, the Hu geodesic is calculated for the topological quotient space $\mathscr{R}^{2n}/W(r)$, where $W(r)$ is defined by the requirement that no vehicles are closer together than some critical Euclidean distance $r$. For autonomous ground vehicles, $\mathscr{R}^2$ must be replaced by a far more topologically complex roadmap space $\mathscr{M}^2$ subject to traffic jams and other 'snowflake' condensation geometries in real time. Geodesics for $n$ vehicles are then in a highly irregular quotient space $\mathscr{M}^{2n}/W(r)$ whose dynamics are subject to phase transitions in vehicle density $\rho$ (Kerner and Klenov 2009; Kerner et al. 2015; Jin et al. 2013) that, we will show, represent cognitive groupoid symmetry breaking. See the Mathematical Appendix for a brief description of groupoids.

In first order, given the factoring out of most of the topological structure by the construction of geodesics in the quotient space $\mathscr{M}^{2n}/W(r)$, the only independent system parameter is the density of vehicles per unit length, which we call $\rho$. Figure 1.1 shows, for streets in Rome, Japan, and Flanders the number of vehicles per unit time as a function of, respectively, vehicles per mile, per kilometer, and percent occupancy: the 'fundamental diagram' of traffic flow. There is a clear 'phase transition' at about 40 vehicles/mile for the former two examples, and at about 10% occupancy for the latter.

We shall extend a simple vehicle density measure to a more complicated unsymmetric density matrix that includes multimodal vehicle indices, an inverse measure of roadway quality, and can be expanded to measures of information channel congestion.

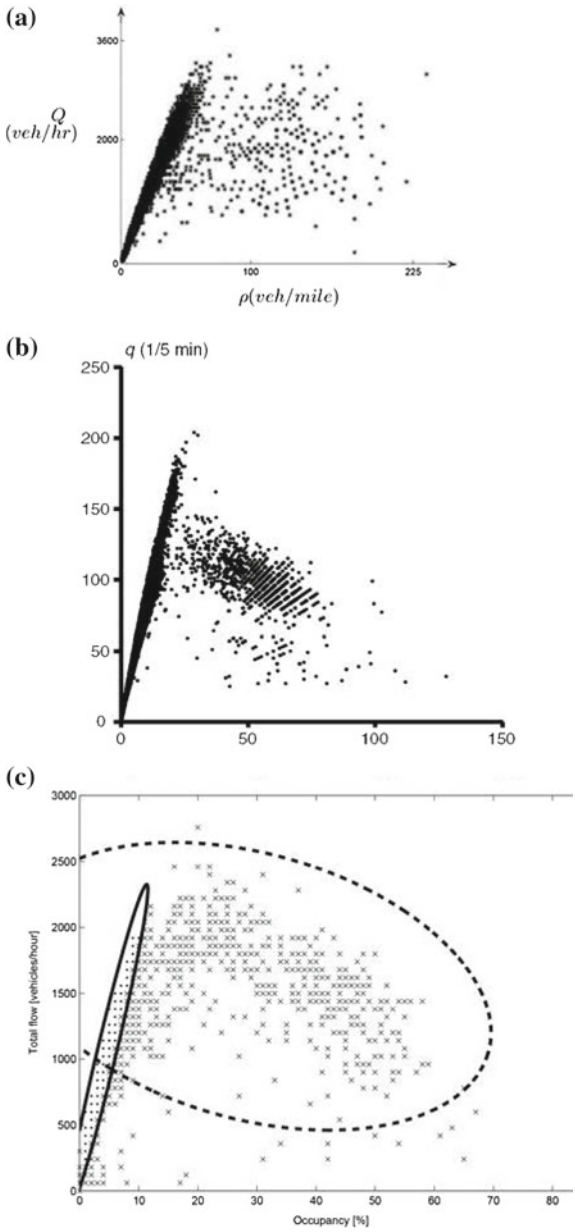


**Fig. 1.1** **a** Vehicles per hour as a function of vehicle density per mile for a street in Rome (Blandin et al. 2011). Both streamline geodesic flow and the phase transition to 'crystallized' turbulent flow at critical traffic density are evident at about 40 v/mi. Some of the states may be 'supercooled', i.e., delayed 'crystallization' in spite of high traffic density. 'Fine structure' can be expected within both geodesic and turbulent modes. **b** One month of data at a single point on a Japanese freeway, flow per five minutes versus vehicles per kilometer. The critical value is about 25 v/km = 39.1 v/mi (Sugiyama et al. 2008). **c** 49 Mondays on a Flanders freeway. The ellipses contain 97.5% of data points for the free flow and congested regimes (Maerivoet and Moor 2006). Breakdown begins just shy of 10% occupancy

Kerner et al. (2015) explicitly apply insights from statistical physics to traffic flow, writing

> In many equilibrium... and dissipative metastable systems of natural science... there can be a spontaneous phase transition from one metastable phase to another metastable phase of a system. Such spontaneous phase transition occurs when a nucleus for the transition appears randomly in an initial metastable phase of the system: The growth of the nucleus leads to the phase transition. The nucleus can be a fluctuation within the initial system phase whose amplitude is equal or larger than an amplitude of a critical nucleus required for spontaneous phase transition. Nuclei for such spontaneous phase transitions can be observed in empirical and experimental studies of many equilibrium and dissipative metastable systems... There can also be another source for the occurrence of a nucleus, rather than fluctuations: A nucleus can be induced by an external disturbance applied to the initial phase. In this case, the phase transition is called an induced phase transition...

A Data Rate Theorem (DRT) approach to stability and flow of autonomous vehicle/traffic control systems, via spontaneous symmetry breaking in cognitive groupoids, generalizes and extends these insights, implying a far more complex picture of control requirements for inherently unstable systems than is suggested by the Theorem itself, or by 'physics' models of phase transition. That is, 'higher order' instabilities can appear. Such systems can require inordinate levels of control information.

More specifically, complicated cognitive systems may remain formally 'stable' in the strict sense of the DRT, but can collapse into a ground state analogous to certain psychopathologies, or even to far more exotic conditions. In biological circumstances, such failures can be associated with the onset of senescence (Wallace 2014, 2015b). Apparently, rapidly responding, and hence almost certainly inherently unstable, command, communications and control systems can display recognizable analogs to senility under fog-of-war demands.

Using these ideas, it becomes possible to explore the interaction of cognitive ground state collapse in autonomous vehicle/intelligent road systems with critical transitions in traffic flow.

Defining 'stability' as the ability to return, after perturbation, to the streamline geodesic trajectory of the embedding, topologically complex, road network, it is clear that individual autonomous vehicles are inherently unstable and require a constant flow of control information for safe operation, unlike aircraft that can, in fact, be made inherently stable by placing the center of pressure well behind the center of gravity. There is no such configuration possible for ground-based vehicles following sinuous road geometries in heavy, shifting, traffic.

Recall Fig. 1.1 Again, the vertical axis shows the number of vehicles per hour, the horizontal, the density of vehicles per mile. The streamline geodesic flow, and deviations from it at critical vehicle density, are evident. Some of the phases may be 'supercooled'—fast-flowing 'liquid' at higher-than-critical densities. Additional 'fine structure' should be expected within both geodesic and turbulent modes.

Classic traffic flow models based on extensions of hydrodynamic perspectives involving hyperbolic partial differential equations (HPDE's) can be analogously factored using the methods of characteristic curves and Riemann invariants—streamlines (Landau and Lifshitz 1987). Along characteristic curves, HPDE's are

projected down to ordinary differential equations (ODE's) that are usually far easier to solve. The ODE solution or solutions can then be projected upward as solutions to the HPDE's. Here, we will show, reduction involves expressing complex dynamics in terms of relatively simple stochastic differential equations and their stability properties. Those stability properties, marking the onset of 'turbulence', will be of central interest.

Taking a somewhat more comprehensive view, cognitive phase transitions in V2V/V2I systems, particularly ground state collapse to some equivalent of 'all possible targets are enemies', should become synergistic with more familiar traffic flow phase transitions to produce truly monumental traffic jams.

A heuristic argument is as follows.

Consider a random network of roads between nodal points—intersections. Taking any two start/destination nodes, in the absence of jamming there will be many possible routes between them, constituting an equivalence class. Moving over all possible start/destination pairs generates a large set of equivalence classes defining a large groupoid, an extension of the idea of a group in which products are not necessarily defined between all possible object pairs (Weinstein 1996). If the average probability of passage falls below a critical value, the Erdos/Renyi 'giant component' that connects across the full network breaks into a set of disjoint connected subcomponents, with 'bottlenecks' at which traffic jams occur marking corridors between them. The large, unjammed, equivalence class groupoid thus undergoes a 'symmetry breaking' phase transition.

Li et al. (2015), in fact, explicitly apply a percolation model to explain this effect for road congestion in a district of Beijing. The underlying road network is shown in Figs. 1.2 and 1.3, a cross section taken during rush hour showing disjoint sections when regions with average velocity below 40% of observed maximum for the road link have been removed. We will later return to giant component models for traffic flow.

But there is more going on here for V2V/V2I systems than simple traffic flow. Below, we will define the cognitive groupoid to be associated with a $C^3$ structure, here a system of autonomous vehicles linked together in a V2V 'swarm intelligence' embedded in the larger vehicle to infrastructure V2I traffic management system. Individual vehicle spacings, speed, acceleration, lane-change, and so on are determined by this encompassing distributed cognitive machine that attempts to optimize traffic flow and safety. The associated individual groupoids are the basic transitive groupoids that build a larger composite groupoid of the cognitive system (Wallace 2015a, 2017). Thus, under declining probability of passage, related to traffic congestion and viewed as a temperature analog, this larger 'vehicle/road' groupoid undergoes a symmetry-breaking transition into a combined cognitive ground state collapse and traffic jam mode—essentially a transition from 'laminar' geodesic to 'turbulent' or 'crystallized' flow. Autonomous vehicle systems that become senile under fog-of-war demands will likely trigger traffic jams that are far different from those associated with human-controlled vehicles. There is no reason to believe that such differences will be benign.

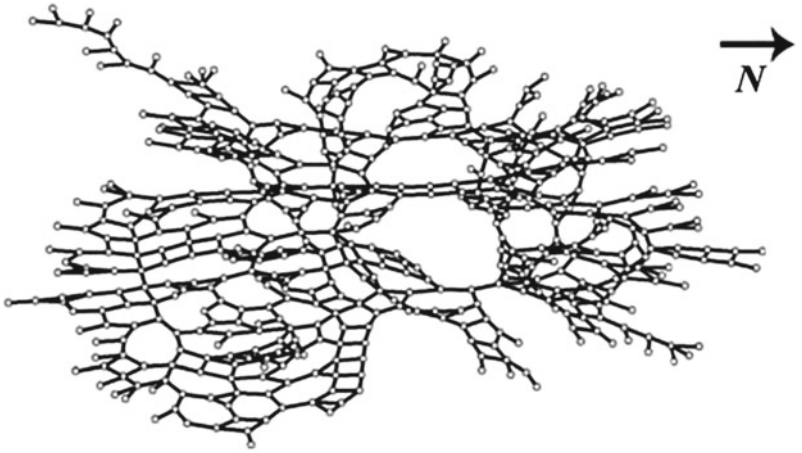


**Fig. 1.2** Adapted from Li et al. (2015). The full road network near central Beijing

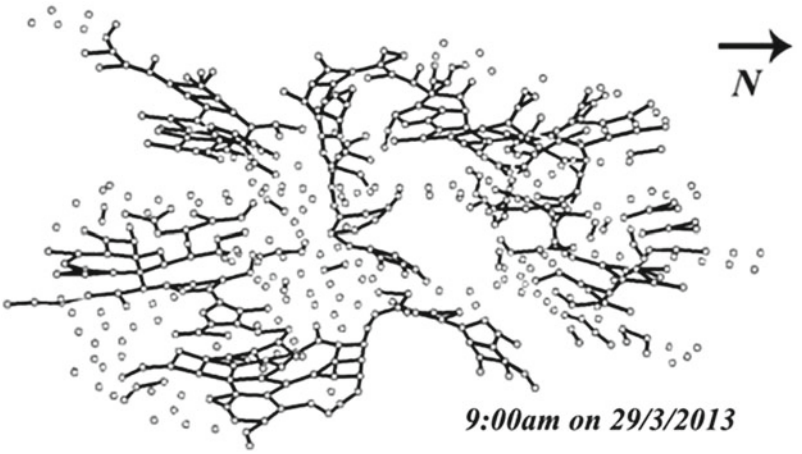


**Fig. 1.3** Adapted from Li et al. (2015). Disconnected subcomponents of the Beijing central road network at rush hour. Sections with average vehicle velocity less than 40% of maximum observed have been removed

We begin the formal development leading to this result with a restatement of the Data Rate Theorem that characterizes the minimum rate of control information needed to ensure stability for an inherently unstable system.

# Chapter 2
# Dynamics of Service Collapse

## 2.1 Introduction

To reiterate a central point, unlike aircraft, that can be constructed to be inherently stable in linear flight by placing the aerodynamic center of pressure sufficiently behind the mechanical center of gravity, the complex nature of road geometry and the local dynamics of vehicular traffic ensure that V2V/V2I systems will be inherently unstable, requiring constant input of control information to prevent crashes, traffic jams, and other tie-ups.

The Data Rate Theorem (Nair et al. 2007) establishes the minimum rate at which externally-supplied control information must be provided for an inherently unstable system to maintain stability. Given the linear expansion near a nonequilibrium steady state, an n-dimensional vector of system parameters at time $t$, $x_t$, determines the state at time $t + 1$ according to the model of Fig. 2.1, so that

$$x_{t+1} = \mathbf{A}x_t + \mathbf{B}u_t + W_t \tag{2.1}$$

where $\mathbf{A}, \mathbf{B}$ are fixed $n \times n$ matrices, $u_t$ is the vector of control information, and $W_t$ is an n-dimensional vector of white noise. The Data Rate Theorem (DRT) under such conditions states that the minimum control information rate $\mathscr{H}$ is determined by the relation

$$\mathscr{H} > \log[|\det[\mathbf{A}^m|]] \equiv a_0 \tag{2.2}$$

where, for $m \leq n$, $\mathbf{A}^m$ is the subcomponent of $\mathbf{A}$ having eigenvalues $\geq 1$. The right hand side of Eq. (2.2) is interpreted as the rate at which the system generates 'topological information'. The proof of Eq. (2.2) is not particularly straightforward (Nair et al. 2007), and the Mathematical Appendix uses the Rate Distortion Theorem (RDT) to derive a more general version of the DRT.



R. Wallace, *Canonical Instabilities of Autonomous Vehicle Systems*,
SpringerBriefs in Computational Intelligence,
https://doi.org/10.1007/978-3-319-69935-6_2

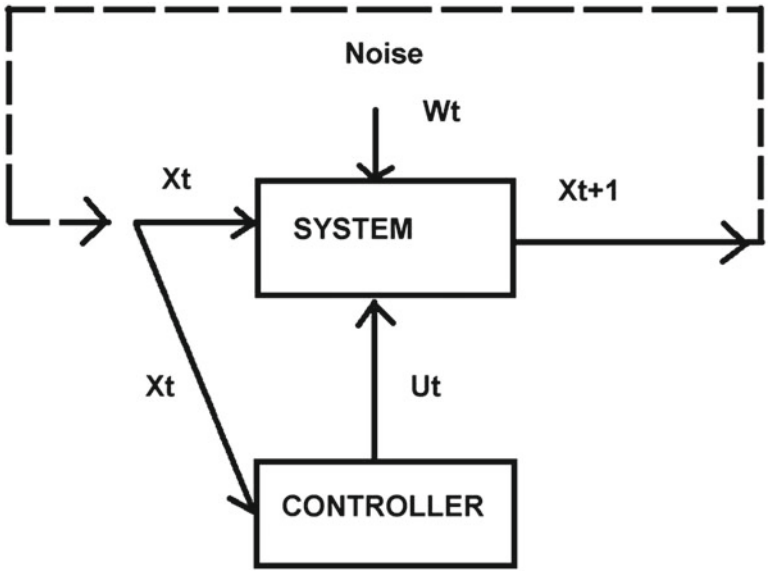


**Fig. 2.1** A linear expansion near a nonequilibrium steady state of an inherently unstable control system, for which $x_{t+1} = \mathbf{A}x_t + \mathbf{B}u_t + W_t$. $\mathbf{A}, \mathbf{B}$ are square matrices, $x_t$ the vector of system parameters at time $t$, $u_t$ the control vector at time $t$, and $W_t$ a white noise vector. The Data Rate Theorem states that the minimum rate at which control information must be provided for system stability is $\mathscr{H} > \log[|\det[\mathbf{A}^m|]$, where $\mathbf{A}^m$ is the subcomponent of $\mathbf{A}$ having eigenvalues $\geq 1$

For a simple traffic flow system on a fixed highway network, the source of 'topological information' is the linear vehicle density $\rho$. The 'fundamental diagram' of traffic flow studies relates the total vehicle flow to the linear vehicle density, shown in Fig. 1.1. A similar pattern can be expected from 'macroscopic fundamental diagrams' that examine multimodal travel networks (Geroliminis et al. 2014; Chiabaut 2015).

Given $\rho$ as the critical traffic density parameter, we can extend Eq. (2.2) as

$$\mathscr{H}(\rho) > f(\rho)a_0 \tag{2.3}$$

where $a_0$ is a road network constant and $f(\rho)$ is a positive, monotonically increasing function. The Mathematical Appendix uses a Black-Scholes model to approximate the 'cost' of $\mathscr{H}$ as a function of the 'investment' $\rho$. The first approximation is linear, so that $\mathscr{H} \approx \kappa_1\rho + \kappa_2$. Expanding $f(\rho)$ to similar order,

$$f(\rho) \approx \kappa_3\rho + \kappa_4 \tag{2.4}$$

the limit condition for stability becomes

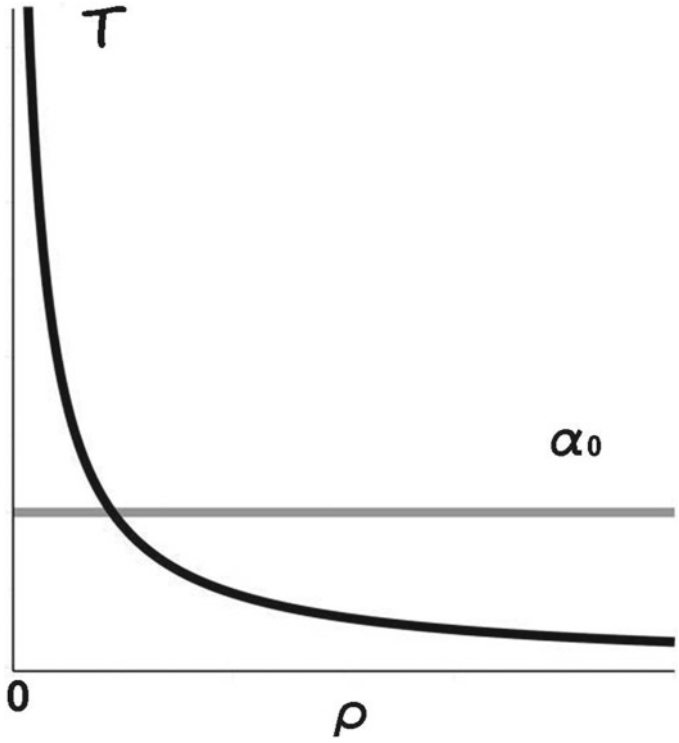


**Fig. 2.2** The horizontal line represents the critical limit $a_0$. If $\kappa_2/\kappa_4 \gg \kappa_1/\kappa_3$, at some intermediate value of linear traffic density $\rho$, the temperature analog $\mathscr{T} \equiv (\kappa_1\rho + \kappa_2)/(\kappa_3\rho + \kappa_4)$ falls below that limit, traffic flow becomes 'supercooled', and traffic jams become increasingly probable

$$\mathscr{T} \equiv \frac{\kappa_1\rho + \kappa_2}{\kappa_3\rho + \kappa_4} > a_0 \tag{2.5}$$

For $\rho = 0$, the stability condition is $\kappa_2/\kappa_4 > a_0$. At large $\rho$ this becomes $\kappa_1/\kappa_3 > a_0$. If $\kappa_2/\kappa_4 \gg \kappa_1/\kappa_3$, the stability condition may be violated at high traffic densities, and instability becomes manifest, as at the higher ranges of Fig. 1.1. See Fig. 2.2.

## 2.2 Multimodal Traffic on Bad Roads

For vehicles embedded in a larger traffic stream there are many other possible critical densities that must interact: different kinds of vehicles per linear mile, V2V/V2I communications bandwidth crowding, and an inverse index of roadway quality that one might call 'potholes per mile', and so on. There is not, then, a simple 'density'

index, but rather a possibly large non-symmetric density matrix $\hat{\rho}$ having interacting components with $\rho_{i,j} \neq \rho_{j,i}$.

Can there still be some scalar '$\rho$' under such complex circumstances so that the conditions of Fig. 2.2 apply? An $n \times n$ matrix $\hat{\rho}$ has $n$ invariants $r_i, i = 1...n$, that remain fixed when 'principal component analysis' transformations are applied to data, and these can be used to construct an invariant scalar measure, using the polynomial relation

$$p(\lambda) = \det(\hat{\rho} - \lambda I) = \lambda^n + r_1\lambda^{n-1} + ... + r_{n-1}\lambda + r_n \tag{2.6}$$

det is the determinant, $\lambda$ is a parameter and $I$ the $n \times n$ identity matrix. The invariants are the coefficients of $\lambda$ in $p(\lambda)$, normalized so that the coefficient of $\lambda^n$ is 1. Typically, the first invariant will be the matrix trace and the last $\pm$ the matrix determinant.

For an $n \times n$ matrix it then becomes possible to define a composite scalar index $\Gamma$ as a monotonic increasing function of these invariants

$$\Gamma = f(r_1, ..., r_n) \tag{2.7}$$

The simplest example, for a $2 \times 2$ matrix, would be

$$\Gamma = m_1 Tr[\hat{\rho}] + m_2 |\det[\hat{\rho}]|$$

for positive $m_i$. Recall that, for $n = 2$, $\mathrm{Tr}[\hat{\rho}] = \rho_{11} + \rho_{22}$ and $\det[\hat{\rho}] = \rho_{11}\rho_{22} - \rho_{12}\rho_{21}$. In terms of the two possible eigenvalues $\alpha_1, \alpha_2$, $\mathrm{Tr}[\hat{\rho}] = \alpha_1 + \alpha_2$, $\det[\hat{\rho}] = \alpha_1\alpha_2$.

Again, an $n \times n$ matrix will have $n$ such invariants from which a scalar index $\Gamma$ can be constructed.

In Eq. (2.5) defining $\mathscr{T}$, $\rho$ is then replaced by the composite density index $\Gamma$,

$$\mathscr{T} = \frac{\kappa_1\Gamma + \kappa_2}{\kappa_3\Gamma + \kappa_4} \tag{2.8}$$

The method is a variant of the 'Rate Distortion Manifold' of Glazebrook and Wallace (2009) or the 'Generalized Retina' of Wallace and Wallace (2013, Sect. 10.1) in which high dimensional data flows can be projected down onto lower dimensional, shifting, tunable 'tangent spaces' with minimal loss of essential information.

## 2.3 The Dynamic Model

We next examine the dynamics of $\mathscr{T}(\Gamma)$ itself under stochastic circumstances. We begin by asking how a control signal $u_t$ in Fig. 2.1 is expressed in the system response $x_{t+1}$. We suppose it possible to deterministically retranslate an observed sequence

of system outputs $X^i = x_1^i, x_2^i, ...$ into a sequence of possible control signals $\hat{U}^i = \hat{u}_0^i, \hat{u}_1^i, ...$ and to compare that sequence with the original control sequence $U^i = u_0^i, u_1^i, ...$, with the difference between them having a particular value under some chosen distortion measure and hence having an average distortion

$$< d >= \sum_i p(U^i) d(U^i, \hat{U}^i) \tag{2.9}$$

where $p(U^i)$ is the probability of the sequence $U^i$ and $d(U^i, \hat{U}^i)$ is the distortion between $U^i$ and the sequence of control signals that has been deterministically reconstructed from the system output.

We can then apply a classic Rate Distortion argument. According to the Rate Distortion Theorem, there exists a Rate Distortion Function, $R(D)$, that determines the minimum channel capacity necessary to keep the average distortion below some fixed limit $D$ (Cover and Thomas 2006). Based on Feynman's (2000) interpretation of information as a form of free energy, it becomes possible to construct a Boltzmann-like pseudoprobability in the 'temperature' $\mathscr{T}$ as

$$dP(R, \mathscr{T}) = \frac{\exp[-R/\mathscr{T}]dR}{\int_0^\infty \exp[-R/\mathscr{T}]dR} \tag{2.10}$$

since higher $\mathscr{T}$ must necessarily be associated with greater channel capacity.

The denominator can be interpreted as a statistical mechanical partition function, and it becomes possible to define a 'free energy' Morse Function (Pettini 2007) $\mathscr{F}$ as

$$\exp[-\mathscr{F}/\mathscr{T}] \equiv \int_0^\infty \exp[-R/\mathscr{T}]dR = \mathscr{T} \tag{2.11}$$

so that $\mathscr{F}(\mathscr{T}) = -\mathscr{T}\log[\mathscr{T}]$.

See the Mathematical Appendix for a brief introduction to Morse Theory.

Then an 'entropy' can also be defined as the Legendre transform of $\mathscr{F}$,

$$\mathscr{S} \equiv \mathscr{F}(\mathscr{T}) - \mathscr{T}d\mathscr{F}/d\mathscr{T} = \mathscr{T} \tag{2.12}$$

The Onsager treatment of nonequilibrium thermodynamics (de Groot and Mazur 1984), can now be invoked, based on the gradient of $\mathscr{S}$ in $\mathscr{T}$, so that a stochastic Onsager equation can be written as

$$\begin{aligned} d\mathscr{T}_t = (\mu d\mathscr{S}/d\mathscr{T})dt + \beta\mathscr{T}_t dW_t = \\ \mu dt + \beta\mathscr{T}_t dW_t \end{aligned} \tag{2.13}$$

where $\mu$ is a diffusion coefficient and $\beta$ is the magnitude of the impinging white noise $dW_t$. Although at first sight the mean for $\mathscr{T}$ would appear to increase at the rate $\mu$,

simulations at high noise show this is simply not true. The stochastic self-stabilization theorem (e.g., Mao 1996, 2007) indicates that unstable differential equations of the form $dx(t)/dt = f(x(t), t)$—for which $x(t)$ 'explodes' as $t \to \infty$—can be stabilized in a stochastic differential equation model $dx_t = f(x_t, t)dt + \sigma x_t dW_t$ if $\sigma$ is sufficiently large and $|f(x, t)| \leq |x|\omega$ for some $\omega > 0$. Then

$$\limsup_{t\to\infty} \frac{1}{t} \log[x(t)] \leq -\frac{\sigma^2}{2} + \omega \tag{2.14}$$

As a consequence, if $\sigma^2/2 > \omega$, then $x(t) \to 0$, according to this model.

Indeed, there is a far more general result for multidimensional systems whose implications we will explore below (Appleby et al. 2008).

Something akin to the Doleans-Dade exponential (Protter 1990) of the Mathematical Appendix emerges by applying the Ito chain rule to $\log(\mathscr{T})$ in Eq. (2.13) (Protter 1990). Via Jensen's inequality for a concave function, the nonequilibrium steady state (nss) expectation of $\mathscr{T}$ then has the lower limit

$$E(\mathscr{T}_t) \geq \frac{\mu}{\beta^2/2} \tag{2.15}$$

In the V2V/V2I context, $\mu$ represents attempts by the system to keep traffic flowing well by raising $\mathscr{T}$, and $\beta$ is the magnitude of a traffic flow/roadway state 'white noise' $dW_t$ contrary to those attempts.

Recall that, in the multimodal extension of the model, the condition for stability is

$$\mathscr{T} \approx \frac{\kappa_1 \Gamma + \kappa_2}{\kappa_3 \Gamma + \kappa_4} > a_0 \tag{2.16}$$

The inference is that sufficient system noise, $\beta$, can drive $\mathscr{T}$ below critical values in Fig. 2.2, triggering a system collapse analogous to a large, propagating traffic jam. Under real world conditions, adequate service will simultaneously raise $\mu$ and lower $\beta$. Nonetheless, Eq. (2.15) is an expectation, *and there will always be some probability that* $\mathscr{T} < a_0$, i.e., that the condition for stability is violated. The system then becomes 'supercooled' and subject to a raised likelihood of sudden, rapidly propagating, traffic jam-like condensations in the sense of Kerner et al. (2015).

It is of some significance that, if the second term in Eq. (2.13) has the plausible form

$$\beta\sqrt{\mathscr{T}_t^2 + \alpha^2} dW_t, \ \alpha > 0 \tag{2.17}$$

so there is intrinsic volatility independent of $\mathscr{T}$, then, applying the Ito expansion to $\log[\mathscr{T}]$, there are two nonequilibrium steady state lower limits:

$$E(\mathscr{T}_t) \geq \frac{\mu \pm \sqrt{\mu^2 - \alpha^2\beta^4}}{\beta^2} \tag{2.18}$$

suggesting, first, the onset of systemic instability if $\alpha\beta^2 \geq \mu$, where $\mu$ incorporates the ability of the system to meet demand. This condition would seem to be independent of, and in addition to, the DRT stability requirement that $\mathscr{T} > a_0$. But further study shows only the larger value solution is actually stable. The lower level either rises to the higher or crashes out to zero in a total system collapse: gridlock. This is probably an observable effect to which we will return below in a section on the 'macroscopic fundamental diagram' describing traffic flow on a network rather than a single road segment.

## 2.4 Multiple Phases of Dysfunction

The DRT argument implies a raised probability of a transition between stable and unstable behavior if the temperature analog $\mathscr{T}(\Gamma)$ falls below a critical value. Kerner et al. (2015), however, argue that traffic flow can be subject to more than two phases. We can recover something similar via a 'cognitive paradigm' like that used by Atlan and Cohen (1998) in their study of the immune system. They view a system as cognitive if it must compare incoming signals with a learned or inherited picture of the world, then actively choosing a response from a larger set of those possible to it. V2V/V2I systems are clearly cognitive in that sense. Such choice, however, implies the existence of an information source, since it reduces uncertainty in a formal way. See Wallace (2012, 2015a, b) for details of the argument.

Given the 'dual' information source associated with the inherently unstable cognitive V2V/V2I system, an equivalence class algebra can be constructed by choosing different system origin states and defining the equivalence of subsequent states at a later time by the existence of a high probability path connecting them to the same origin state. Disjoint partition by equivalence class, analogous to orbit equivalence classes in dynamical systems, defines a symmetry groupoid associated with the cognitive process (Wallace 2012). Again, groupoids are generalizations of group symmetries in which there is not necessarily a product defined for each possible element pair (Weinstein 1996), for example in the disjoint union of different groups.

The equivalence classes across possible origin states define a set of information sources dual to different cognitive states available to the inherently unstable V2V/V2I system. These create a large groupoid, with each orbit corresponding to a transitive groupoid whose disjoint union is the full groupoid. Each subgroupoid is associated with its own dual information source, and larger groupoids must have richer dual information sources than smaller.

Let $X_{G_i}$ be the system's dual information source associated with groupoid element $G_i$. Given the argument leading to Eqs. (2.5–2.7), we construct another Morse Function (Pettini 2007) as follows.

Let $H(X_{G_i}) \equiv H_{G_i}$ be the Shannon uncertainty of the information source associated with the groupoid element $G_i$. We define another pseudoprobability as

$$P[H_{G_i}] \equiv \frac{\exp[-H_{G_i}/\mathscr{T}]}{\sum_j \exp[-H_{G_j}/\mathscr{T}]} \tag{2.19}$$

where the sum is over the different possible cognitive modes of the full system.

Another, more complicated, 'free energy' Morse Function $F$ can then be defined as

$$\exp[-F/\mathscr{T}] \equiv \sum_j \exp[-H_{G_j}/\mathscr{T}] \tag{2.20}$$

or, more explicitly,

$$F = -\mathscr{T} \log[\sum_j \exp[-H_{G_j}/\mathscr{T}]] \tag{2.21}$$

As a consequence of the groupoid structures associated with complicated cognition, as opposed to a 'simple' stable-unstable control system, we can now apply an extension of Landau's version of phase transition (Pettini 2007). Landau saw spontaneous symmetry breaking as representing phase change in physical systems, with the higher energies available at higher temperatures being more symmetric. The shift between symmetries is highly punctuated in the temperature index, here the 'temperature' analog of Eq. (2.5), in terms of the scalar construct $\Gamma$, but in the context of groupoid rather than group symmetries. Usually, for physical systems, there are only a few phases possible. Kerner et al. (2015) recognize three phases in ordinary traffic flow, but V2V/V2I systems may have relatively complex stages of dysfunction, with highly punctuated transitions between them as various density indicies change and interact.

Later we will explore sufficient conditions for the pathological ground state to 'lock-in' and become highly resistant to managerial intervention, that is, for a highly persistent large-scale traffic jam. Such 'lock-in' may help explain often-observed hysteresis effects in traffic flow, and the general intractability of the Macroscopic Fundamental Diagram for certain road networks.

In this context, Birkhoff's (1960, p.146) perspective on the central role of groups in fluid mechanics is of considerable interest:

> [Group symmetry] underlies the entire theories of dimensional analysis and modeling. In the form of 'inspectional analysis' it greatly generalizes these theories... [R]ecognition of groups... often makes possible reductions in the number of independent variables involved in partial differential equations... [E]ven after the number of independent variables is reduced to one... the resulting system of ordinary differential equations can often be integrated most easily by the use of group-theoretic considerations.

We argue here that, for 'cognitive fluids' like vehicle traffic flows, groupoid generalizations of group theory become central.

Decline in the richness of control information, or in the ability of that information to influence the system as measured by the 'temperature' index $\mathscr{T}(\Gamma)$, can lead to punctuated decline in the complexity of cognitive process possible within the $C^3$ system, driving it into a ground state collapse that may not be actual 'instability'

but rather a kind of dead zone in which, using the armed drone example, 'all possible targets are enemies'. This condition represents a dysfunctionally simple cognitive groupoid structure roughly akin to certain individual human psychopathologies (Wallace 2015a).

It appears that, for large-scale autonomous vehicle/intelligent infrastructure systems, the ground state dead zone involves massive, propagating tie-ups that far more resemble power network blackouts than traditional traffic jams. Again, the essential feature is the role of composite system 'temperature' $\mathscr{T}(\Gamma)$. Most of the topology of the inherently unstable vehicles/roads system will be 'factored out' via the construction of geodesics in a topological quotient space, so that $\mathscr{T}(\Gamma)$ inversely indexes the rate of topological information generation for an extended DRT.

Lowering the 'temperature' $\mathscr{T}$ forces the system to pass from high symmetry 'free flow' to different forms of 'crystalline' structure—broken symmetries representing platoons, shock fronts, traffic jams, and more complicated system-wide patterns of breakdown such as hysteresis.

In the next chapter the underlying dynamics are treated in finer detail from different perspectives, viewing the initial phase transition as a transition from free flow to 'flock' structures like those studied in 'active matter' physics. Indeed, the traffic engineering perspective is quite precisely the inverse of mainstream active matter studies, which Ramaswamy (2010) describes as follows:

> It is natural for a condensed matter physicist to regard a coherently moving flock of birds, beasts, or bacteria as an orientationally ordered phase of living matter. ...[M]odels showed a nonequilibrium phase transition from a disordered state to a flock with long-range order... in the particle velocities as the noise strength was decreased or the concentration of particles was raised.

In traffic engineering, the appearance of such 'long range order' is the first stage of a traffic jam (Kerner and Klenov 2009; Kerner et al. 2015), a relation made explicit by Helbing (2001, Sect. 6) in his comprehensive review of traffic and related self-driven many-particle systems.

While flocking and schooling have obvious survival value against predation for animals in three-dimensional venues, long-range order—aggregation—among blood cells flowing along arteries is a blood clot and can be rapidly fatal.

# Chapter 3
# The 'Macroscopic Fundamental Diagram'

## 3.1 Introduction

A long line of work summarized by Cassidy et al. (2011) attempts to extend the idea of a fundamental diagram for a single road to a full transport network. As they put it,

> Macroscopic fundamental diagrams (MFDs)... relate the total time spent to the total distance traveled... It is proposed that these macrolevel relations should be observed if the data come from periods when all lanes on all links throughout the network are in either the congested or the uncontested regime...

Some evidence exists for the MFD under specific circumstances. Figure 3.1, from Geroliminis and Daganzo (2008) shows the average traffic flow versus occupancy for downtown Yokohama, where major intersections are centrally controlled by multiphase traffic signals with a cycle time that responds to traffic conditions, 110–120 s at night, 130–140 s during the day.

However, Fig. 1.3 suggests why MFDs cannot be constructed in general: Congested and free flowing sections of traffic networks will often, and perhaps usually, coexist in an essentially random manner depending on local traffic densities. Figure 3.2, adapted from Geroliminis and Sun (2011a), further demonstrates the limitations of the MFD approach. It examines the flow, in vehicles/5min intervals, versus percent occupancy over a three day period for the Minnesota Twin Cities freeway network that connects St. Paul and Minneapolis. See Fig. 1 of their paper for details of the road and sensor spacing. Evidently, while the unconstrained region of occupancy permits characterization of a geodesic mode, both strong hysteresis and phase transition effects are evident after about 8% occupancy, analogous to the 'nucleation' dynamics of Fig. 1.1 at high traffic density. Again, as in Fig. 1.1 'fine structure' should be expected within both geodesic and turbulent modes, depending on local parameters.

Daganzo et al. (2010) further find that MFD flow, when it can be characterized at all, will become unstable if the average network traffic density is sufficiently high. They find that, for certain network configurations, the stable congested state



R. Wallace, *Canonical Instabilities of Autonomous Vehicle Systems*,
SpringerBriefs in Computational Intelligence,
https://doi.org/10.1007/978-3-319-69935-6_3

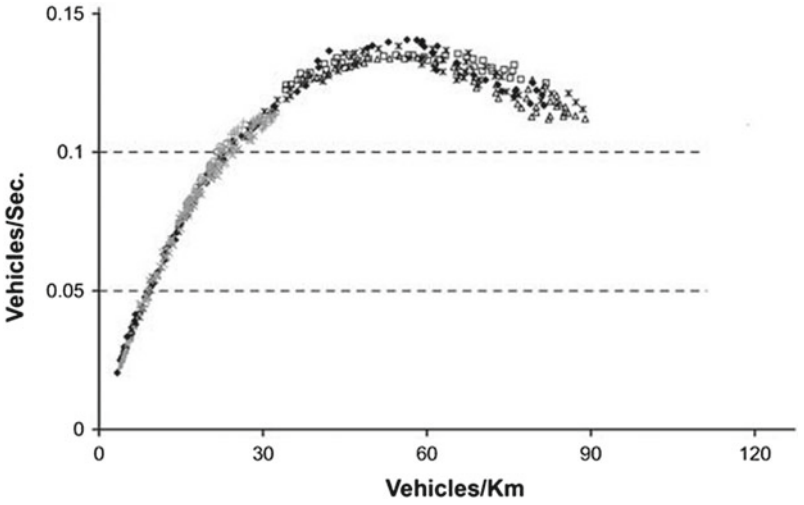


**Fig. 3.1** Adapted from Geroliminis and Daganzo (2008). Average traffic flow versus occupancy (v/km) for a set of detectors in downtown Yokohama over two days. Major intersections are centrally controlled by multiphase traffic signals that respond to traffic conditions. The stability of traffic flow on the road network is thus critically dependent on the stability of the embedding control network

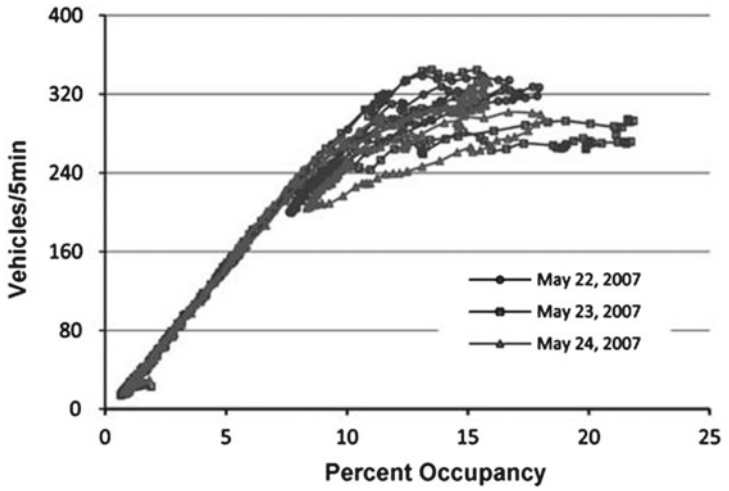


**Fig. 3.2** Adapted from Geroliminis and Sun (2011a). Breakdown of the macroscopic fundamental diagram for the freeway network connecting St. Paul and Minneapolis at high vehicle densities. Both nucleation and hysteresis effects are evident, showing the fine structure within the turbulent mode. As in Fig. 1.1c, breakdown begins near 8–10% occupancy. Unlike Fig. 3.1, here there is no network of active control signals

> ...is one of complete gridlock with zero flow. It is therefore important to ensure that in real-world applications that a network's [traffic] density never be allowed to approach this critical value.

Geroliminis and Sun (2011b) caution that

> ...[F]reeway networks do not have well-defined MFDs between network flow and density, as these networks have topological or control characteristics that are different from arterial networks... [R]esearch is needed in different types of networks to understand how variations in the topology/structure of the networks can affect the shape, the scatter and the existence of an MFD... MFD's should not be universally expected... a careful analysis is necessary before... control strategies/policies are introduced based on monitoring aggregated variables.

Daqing et al. (2014) examine the dynamic spread of traffic congestion on the Beijing central road network. They characterize the failure of a road segment to be a traffic velocity less than 20 km/hr and use observational data to define a spatial correlation length in terms of the Euclidean distances between failed nodes. Adapting their results, Fig. 3.3 shows the daily pattern of the correlation length of cascading traffic jams over a 9 day period. The two commuting maxima are evident, and greatest correlation lengths reach the diameter of the main part of the city. Even at rush hour,

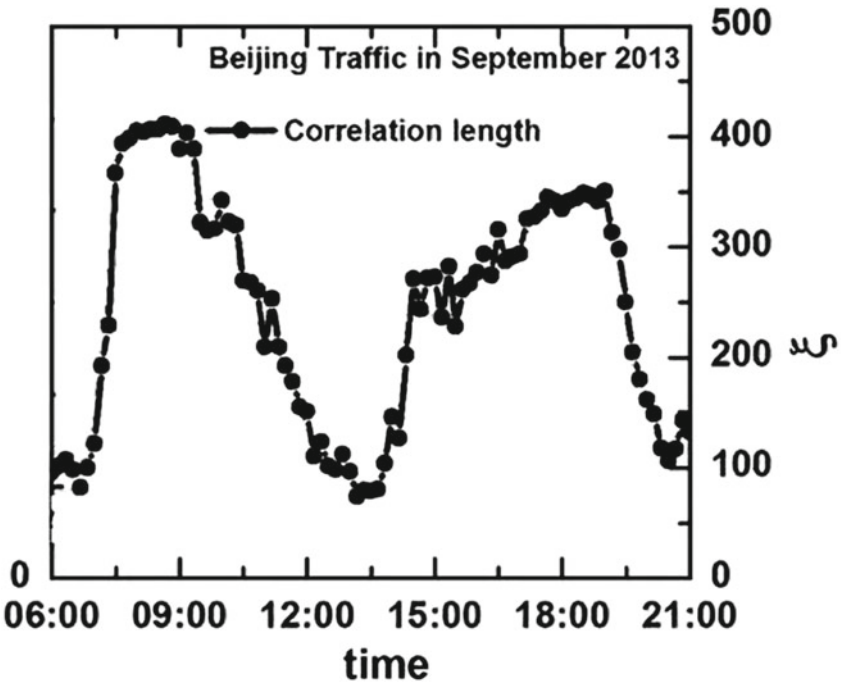


**Fig. 3.3** Adapted from Daqing et al. (2014). Daily cycle of traffic jam correlation length over a 9 day period in central Beijing. The maxima cover most of the central city. For rush hour, no macroscopic fundamental diagram can be defined since the region is characterized by a patchwork of free and congested parts, as shown in Fig. 1.3

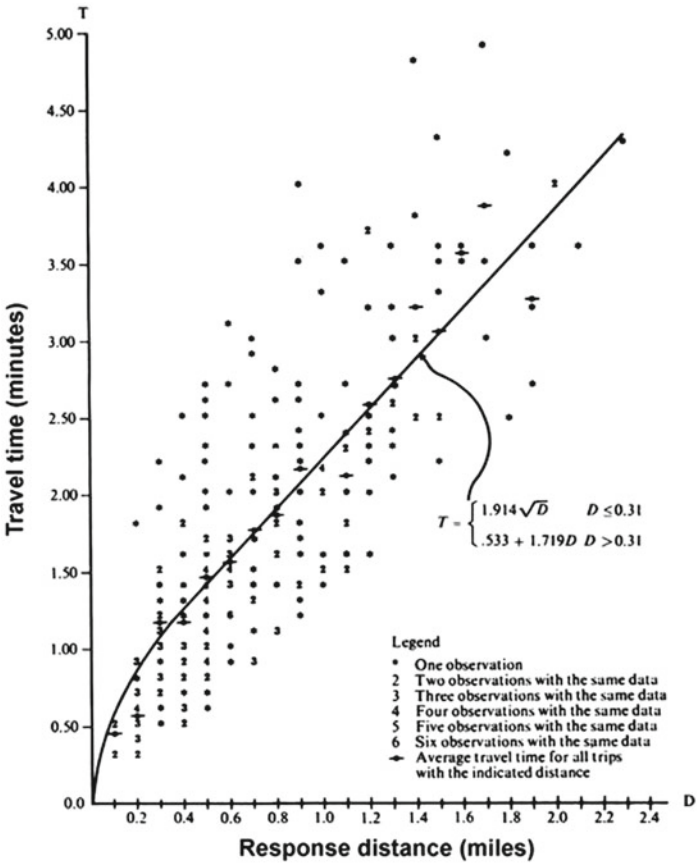


**Fig. 3.4** Adapted from Fig. 6.4 of Rand (1979). Relation between fire company travel time and response distance for the full Trenton, NJ road network, 1975. The Rand Fire Project collapsed evident large-scale traffic turbulence into a simple 'square root-linear' model used to design fire service deployment policies in high fire incidence, high population density neighborhoods of many US cities, including the infamous South Bronx. The impacts were literally devastating (Wallace and Wallace 1998)

no MFD can be defined, as, according to Fig. 1.3, the network will be a dynamic patchwork of free and congested components.

Figure 3.4, adapted from Rand (1979, Fig. 6.4), provides a disturbing counterexample to these careful empirical and theoretical results on network traffic flow, one with unfortunate results. Summarizing observations carried out by the Rand Fire Project, it represents a repeated sampling of 'travel time versus distance' for the full Trenton NJ road network in 1975 under varying conditions of time-of-day, day-of-week, weather, and so on, by fire companies responding to calls for service. This was an attempt to create a Macroscopic Fundamental Diagram in the sense used above, but without any reference at all to traffic density.

Indeed, fire service responses are a traffic flow 'best case' as fire units are permitted to bypass one-way restrictions, traffic lights, and so on, and usually able to surmount even the worst weather conditions. In spite of best-case circumstances, the scatterplot evidently samples whole-network turbulent flow, not unlike that to the right of the local geodesic in Figs. 1.1 and 3.2, part of a single street and a highway network, respectively, and consistent with the assertions of Cassidy et al. (2011) that MFD relations can only be defined under very restrictive conditions, i.e., either complete free flow or full network congestion.

The Rand Fire Project, when confronted with intractable whole-network traffic turbulence, simply collapsed the data onto a 'square root-linear' relation, as indicated on the figure. The computer models resulting from this gross oversimplification were used to determine fire service deployment strategies for high fire incidence, overcrowded neighborhoods in a number of US cities, with literally devastating results and consequent massive impacts on public health and public order. Wallace and Wallace (1998), produced under an Investigator Award in Health Policy Research from the Robert Wood Johnson Foundation, documents the New York City case history. The Rand models are still in use by the New York City Fire Department, for political purposes outlined in that analysis.

## 3.2 Intractability of the MFD

Why is the macroscopic fundamental diagram so apparently intractable in one case, but not in another? Some insight is gained by recognizing that road networks are inherently two dimensional in their *populations* as well as their geometries. That is, a road network, as opposed to a road segment, can be viewed as having distinct populations of network nodes and vehicles. This is different from macroscopic electrical systems in which the electrons are not, and cannot be, counted. We can, at least to first order, study a traffic jam in terms of interacting populations as follows.

Let $X$ be the proportion of road network nodes suffering a jam, and $Y$ be the proportion of vehicles in a jam. These populations, of course, interact, and the simplest model is one of cross-influence:

$$\begin{aligned} dX/dt &= \mu_1 Y(1-X) - \gamma_1 X \\ dY/dt &= \mu_2 X(1-Y) - \gamma_2 Y \end{aligned} \tag{3.1}$$

where $\gamma_1$ is the average rate at which a node is cleared, and $\gamma_2$ the average rate at which a vehicle clears a jam. The $\mu_i$ represent 'contagion' effects.

The essential point, again, is that, for road networks, and unlike electrical and hydrodynamic networks, individual vehicles and individual nodes can interact strongly.

At nonequilibrium steady state

$$X = \frac{\mu_1\mu_2 - \gamma_1\gamma_2}{\mu_2(\mu_1 + \gamma_1)}$$
$$Y = \frac{\mu_1\mu_2 - \gamma_1\gamma_2}{\mu_1(\mu_2 + \gamma_2)} \tag{3.2}$$

If $\mu_1\mu_2 < \gamma_1\gamma_2$, then $X, Y \to 0$, and no jam can propagate.

We can bring closure to the model by assuming that the $\mu_i$ are monotonic increasing, and the $\gamma_i$ monotonic decreasing, in the traffic density index $\rho$, the multimodal composite $\Gamma$ from Eq. (2.7), or the 'percent occupancy' from Fig. 3.2. The nss values of $X$ and $Y$ then take an inverted J form, rising above zero at threshold and asymptotically approaching 1. Almost exactly similar functional forms for 'packet delay' versus 'average transmission rate' can be found in the computer network studies of Sole and Valverde (2001, Fig. 2a), and Ohira and Sawatari (1998, Figs. 1 and 2). Figure 3.5 shows the form of the relation for $\mu_i = \rho, \gamma_i = 1/\rho$. This is a qualitative form characteristic of network loading across a variety of models.

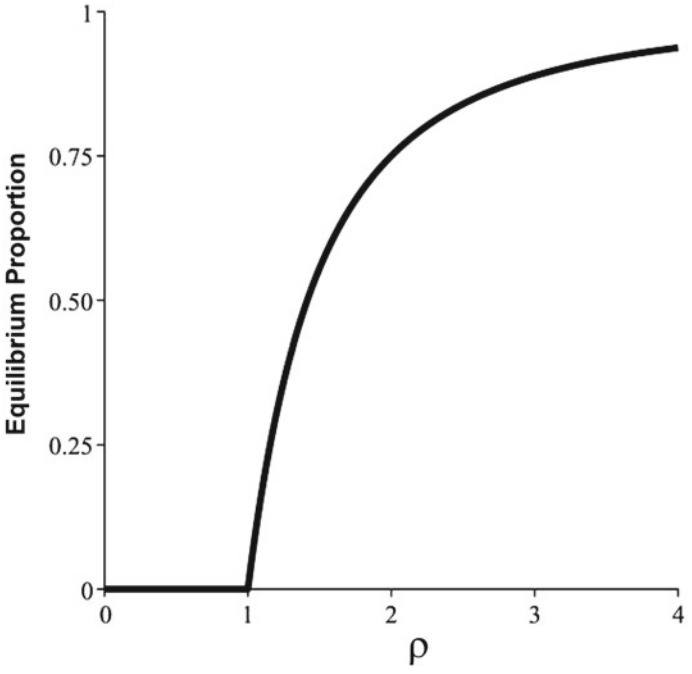


**Fig. 3.5** Equilibrium proportion of jammed vehicles, taking $\mu_i = \rho, \gamma_i = 1/\rho$. The relation is then $X = 0$ if $\rho \leq 1$, $X = (\rho^2 - 1/\rho^2)/(\rho(\rho + 1/\rho))$ if $X > 1$. This 'inverted J' form will repeat across different models of network congestion

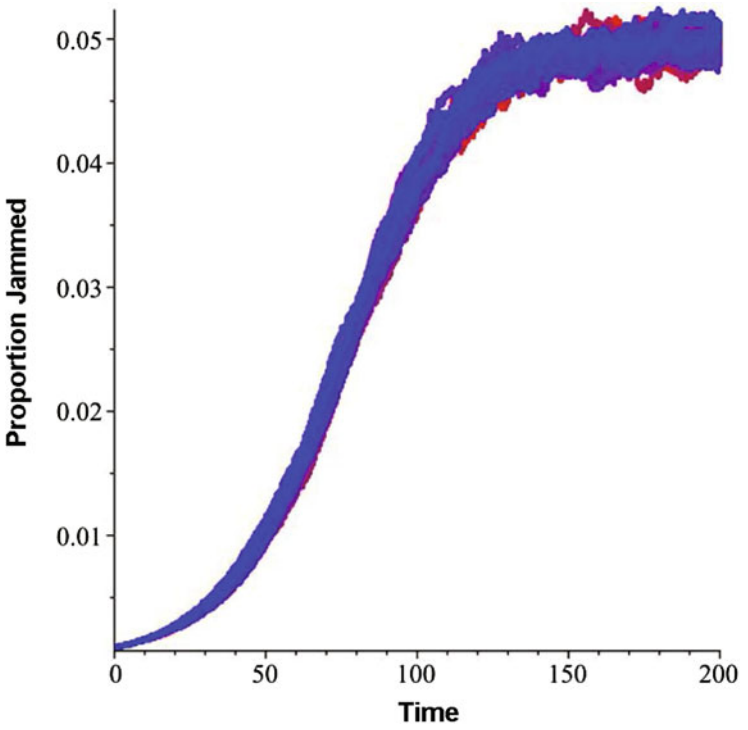


**Fig. 3.6** Thirty simulations of Eq. (3.3) using a cross-influence noise ±0.01. The time dependence is just that of the deterministic model plus some minor diffusion. Red = X, blue = Y

But there is more going on here, and the subtleties help explain the difference between Figs. 3.1 and 3.2.

Taking $\mu_i = 1, \gamma_1 = 1, \gamma_2 = 0.9$, the nss values of $X$ and $Y$ are, respectively, 0.050, 0.0526.... We perturb this system with white noise, using the ItoProcess function available in the computer algebra program Maple, performing 30 simulations of the SDE system

$$\begin{aligned} dX_t &= [Y_t(1 - X_t) - X_t]dt - 0.01Y_t dW_t^1 \\ dY_t &= [X_t(1 - Y_t) - 0.9Y_t]dt + 0.01X_t dW_t^2 \end{aligned} \tag{3.3}$$

as shown in Fig. 3.6.

The result is simply the approach to the nss, with some diffusional fuzzing.

Next, we add a significant amount of noise:

$$\begin{aligned} dX_t &= [Y_t(1 - X_t) - X_t]dt - 0.4Y_t dW_t^1 \\ dY_t &= [X_t(1 - Y_t) - 0.9Y_t]dt + 0.4X_t dW_t^2 \end{aligned} \tag{3.4}$$

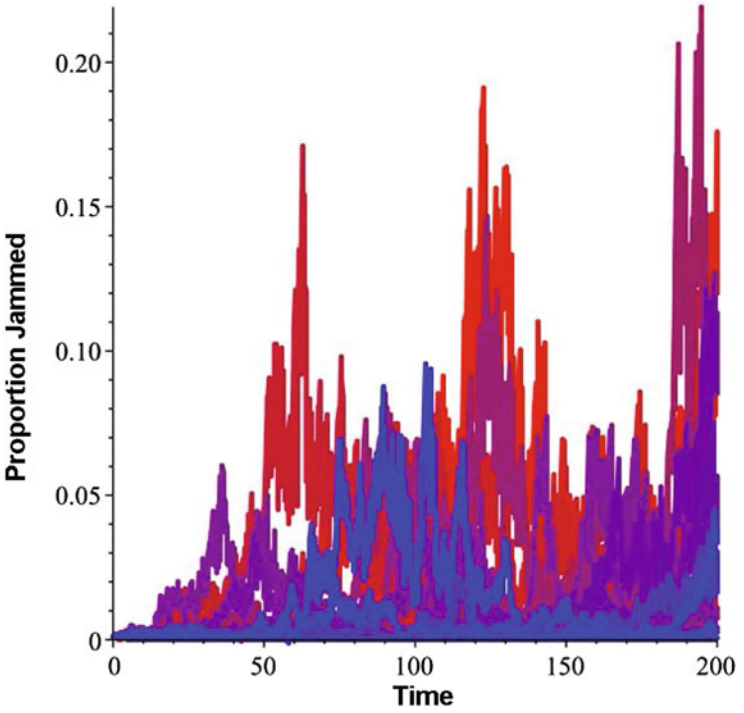


**Fig. 3.7** The same as Fig. 3.6, but with cross-noise ±0.4, forty times as strong. The system now increasingly diverges from the endemic level of approximately 5%

Figure 3.7 shows the outcome. For sufficient added cross-noise of different sign, the system does not converge on the nss of about 5%, but undergoes repeated, and indeed progressively rising, excursions. While the underlying parameters that define the low 'endemic' level in the deterministic model remain the same, the added noise is now seriously destabilizing.

It seems obvious that onset of such instability will occur at progressively lower noise levels as such traffic load indices as $\rho$, $\Gamma$ or 'percent occupancy' increase.

The mechanisms for this dynamic have only recently become clear and greatly extend the results of Eq. (2.14).

A function $f$ is said to be locally Lipshitz if, for $f$ from $S \subset R^n \rightarrow R^m$, there is a constant $C$ such that $||f(y) - f(x)|| \leq C||y - x||$ for all $y \in S$ that are sufficiently near to $x$. Then Appleby et al. (2008) show that, for any such function $f$, a function $g$ can always be found so that the perturbed SDE

$$dX_t = f(X_t)dt + g(X_t)dW_t \tag{3.5}$$

either stabilizes an unstable equilibrium of $f$, or, for dimension $\geq 2$, destabilizes a stable equilibrium. In one dimension, equations remain only stabilizable by noise.

Vehicles on roads, unlike molecules in pipes, can be represented in terms of two or more macroscopic, interacting populations. Arterial and freeway networks have fundamental structural differences. For freeway networks, chaos almost surely follows at sufficiently high vehicle densities, rendering the 'macroscopic fundamental diagram' a concept useful only at very low traffic loadings. Arterial networks can actively direct traffic flow perturbations—'noise'—differently, and will sometimes jam at high densities without chaos, giving a well-defined 'inverted U' MFD.

A second way of viewing the failure of traffic flow on a road network is, conceptually, somewhat similar to describing the propagation of a signal via the Markov 'network dynamics' formalism of Wallace (2016a) or Gould and Wallace (1994). This is an approach that might be used to empirically identify geodesic eigenmodes of real road network systems under different conditions, as opposed to individual vehicle dynamics or flow on a single road. Zhang (2015), in fact, uses a similar Markov method to examine taxicab GPS data for transit within and between 12 empirically-identified 'hot zones' in Shanghai, determining the network probability-of-contact matrix (POCM) and its equilibrium distribution.

Following Gould and Wallace (1994), the spread of a 'signal' on a particular network of interacting sites—between and within—is described at nonequilibrium steady state in terms of an equilibrium distribution $\varepsilon_i$ 'per unit area' $A_i$ of a Markov process, where $A$ scales with the different 'size' of each node, taken as distinguishable by a scale variable $A$ (for example number of entering streets or average total traffic flow) as well as by its 'position' $i$ or the associated POCM. The POCM is then normalized to a stochastic matrix $\mathbf{Q}$ having unit row sums, and the vector $\varepsilon$ calculated as $\varepsilon = \varepsilon\mathbf{Q}$

There is a vector set of dimensionless network flows $\mathscr{X}_t^i$, $i = 1, ..., n$ at time $t$. These are each determined by some relation

$$\mathscr{X}_t^i = g(t, \varepsilon_i / A_i) \tag{3.6}$$

Here, $i$ is the index of the node of interest, $\mathscr{X}_t^i$ is the corresponding dimensionless scaled i-th signal, $t$ the time, and $g$ an appropriate function. Again, $\varepsilon_i$ is defined by the relation $\varepsilon = \varepsilon\mathbf{Q}$ for a stochastic matrix $\mathbf{Q}$, calculated as the network probability-of-contact matrix between regions, normalized to unit row sums. Using $\mathbf{Q}$, we have broken out the underlying network topology, a fixed between-and-within travel configuration weighted by usage that is assumed to change relatively slowly on the timescale of observation compared to the time needed to approach the nonequilibrium steady state distribution.

Since the $\mathscr{X}$ are expressed in dimensionless form, $g$, $t$, and $A$ must be rewritten as dimensionless as well giving, for the monotonic increasing (or threshold-triggered) function $F$

$$\mathscr{X}_\tau^i = G[\tau, \frac{\varepsilon_i}{A_i} \times \mathscr{A}_\tau] \tag{3.7}$$

where $\mathscr{A}_\tau$ is the value of a 'characteristic area' variate that represents the spread of the perturbation signal—evolving into a traffic jam under worst-case conditions—at (dimensionless) characteristic time $\tau = t/T_0$.

$G$ may be quite complicated, including dimensionless 'structural' variates for each individual geographic node $i$. The idea is that the characteristic 'area' $\mathscr{A}_\tau$ grows according to a stochastic process, even though $G$ may be a deterministic mixmaster driven by systematic local probability-of-contact or flow patterns. Then the appropriate model for $\mathscr{A}_\tau$ in a spreading traffic jam resembles Eq. (2.15), with $x$ replaced by $\mathscr{A}$ and $t$ by $\tau$. But, for the network, $\mathscr{A}_\tau$ must have a vehicle density threshold condition like Eq. (3.2) for large-scale propagation of a traffic jam across the full network—something that would look very similar to the spread of a power blackout.

A simple example.

A characteristic area cannot grow indefinitely, and we invoke a 'carrying capacity' for a jam on the network under study, say $K > 0$. An appropriate SDE is then

$$d\mathscr{A}_\tau = [\mu\rho\mathscr{A}_\tau(1 - \mathscr{A}_\tau/K)]d\tau + \sigma\mathscr{A}_\tau dW_\tau \tag{3.8}$$

where we take '$\rho$' as representing vehicle density, percent occupancy, or the composite multimodal traffic/street quality index $\Gamma$.

Using the Ito chain rule on $\log(\mathscr{A})$, as a consequence of the added Ito correction factor and the Jensen inequality for a concave function,

$$\begin{aligned} E(\mathscr{A}) &\to 0, \quad \mu\rho < \sigma^2/2 \\ E(\mathscr{A}) &\geq K(1 - \frac{\sigma^2}{2\mu\rho}), \quad \mu\rho \geq \sigma^2/2 \end{aligned} \tag{3.9}$$

Figure 3.8 shows the form of this relation, which is similar to what would be expected from introducing density dependence into Eq. (3.2), e.g., $\mu_i \propto \rho$, $\gamma_i \propto 1/\rho$.

Equation (3.9) differs in an important aspect from Eq. (3.2). It represents the lower limit of an expectation that can vary greatly and unpredictably above the threshold traffic density. As a consequence, determination of a Macroscopic Fundamental Diagram becomes highly problematic, according to this model. Indeed, a nonequilibrium steady state calculation finds the variance of $\mathscr{A}$ growing at a rate greater than $\sigma^4$. This is done using the Ito Chain Rule to calculate $d\mathscr{A}^2$ from Eq. (3.8), remembering that the variance is simply $E(\mathscr{A}^2) - E(\mathscr{A})^2$, and imposing the condition that $d/dt \to 0$.

A third approach to the MFD problem is via classic network theory, adapting the percolation theory example of Li et al. (2015). We first view a road net as a random graph made up of nodes at which roads intersect and the 'edges' which connect them. Edges are identified as 'Open' if they are in free flow, and 'Closed' if congested. Suppose the road net graph has $M$ vertices and $m = (1/2)aM$ closed edges chosen at random. Corless et al. (1996) show that, for $a > 1$, the road net graph almost surely has a giant connected component having approximately $g(a)M$ vertices with


**Fig. 3.8** Lower limit of the expectation for the characteristic area of a traffic jam as a function of a traffic density measure. The expected value will be larger than this, and can vary unpredictably, making the estimation of a Macroscopic Fundamental Diagram impossible above the threshold density

$$g(a) = 1 + W(-a\exp[-a])/a \tag{3.10}$$

where $W$ is the Lambert-W function defined implicitly by the relation

$$W(x)\exp[W(x)] = x \tag{3.11}$$

See Fig. 3.9, which should be compared with Fig. 3.8.

Real networks, however, deviate from random graphs. Typically, the degree distribution, the probability of $k$ linkages between vertices, often follows some power law $P(k) \approx k^{-\gamma}$ rather than the Poisson distribution of random networks, i.e., $P(k) = a^k \exp[-a]/k!,\ k \geq 0$. Molloy and Reed (1995, 1998) show that, for a random graph with degree distribution $P(k)$, an infinite cluster—here a traffic jam—emerges almost surely when

$$Q \equiv \sum_{k\geq 1} k(k-2)P(k) > 0 \tag{3.12}$$

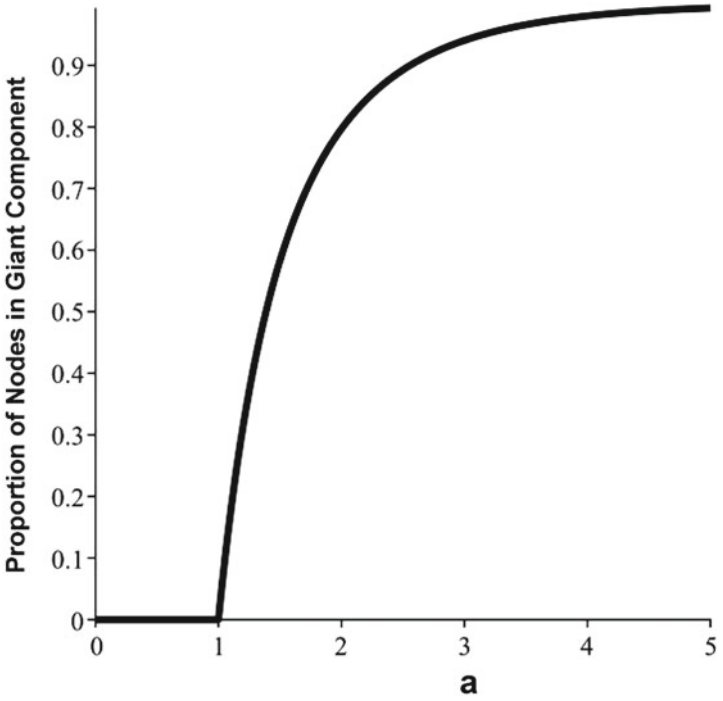


**Fig. 3.9** Relative size of the largest connected component of jammed roads for a random graph. Compare with Fig. 3.8. The traffic jam grows very sharply in extent after criticality is reached

It is possible to extend the Erdos/Renyi threshold results to 'semirandom' graphs. Luczak (1990) shows that almost all random graphs with a fixed degree smaller than two have a unique giant cluster.

The essential point is that, as Newman et al. (2001) show, giant components are ubiquitous, even for nonrandom networks, with the main influence being on the location of the threshold for 'explosion' and the magnitude of the 'topping out' limit.

Coming, in a sense, full circle, Bottcher et al. (2017) examine critical behaviors in network contagion dynamics, finding something similar to what was explored in Sect. 3.2, and a three-component phase diagram analogous to the Kerner model of traffic flow (Kerner et al. 2015; Kerner and Klenov 2009). It might be argued that such 'graph theory' networks are inherently at least two dimensional, characterized by interacting populations of 'nodes' and 'edges', and thus necessarily subject to the kind of stabilization/destabilization described under the Stochastic Stabilization Theorem (Appleby et al. 2008), depending most specifically on the details of the interaction mechanism. Figure 2 of Bottcher et al. seems to present dynamics roughly consonant with those of Figs. 3.6 and 3.7 here.

## 3.3 Hysteresis Lock-In of a Pathological Mode

Sufficient conditions for the stability of the hypercondensed pathological 'ground state' cognitive phase discussed above, providing another model of hysteresis in traffic flow like that shown in Figs. 3.2 and 3.4, can be explored using the methods of Wallace (2016a). Given a vector of parameters characteristic of, and driving, that phase, say $\mathbf{J}$, measuring deviations from a nonequilibrium steady state, the 'free energy' analog $F$ in Eq. (2.21) can be used to define a new 'entropy' scalar as the Legendre transform

$$\mathscr{S} \equiv F(\mathbf{J}) - \mathbf{J} \cdot \nabla_{\mathbf{J}} F \tag{3.13}$$

Then a first-order dynamic equation follows using a stochastic version of the Onsager formalism from nonequilibrium thermodynamics (de Groot and Mazur 1984)

$$dJ_t^i = (\sum_k \mu_{i,k} \partial \mathscr{S} / \partial J_t^k) dt + \sum_k \sigma_i^k J_t^i dB_t^k \tag{3.14}$$

where $\mu_{i,k}$ defines a diffusion matrix, the $\sigma_i$ are parameters, and the $dB_t^k$ represent noise that may be colored, i.e., not the usual Brownian motion under undifferentiated white noise.

We suppose it possible to factor out $J^i$ so that Eq. (3.14) can be expressed as

$$dJ_t^i = J_t^i dY_t^i \tag{3.15}$$

where $Y_t^i$ is now a stochastic process.

Equation (3.15) can then be solved for the expectation of $J$ in terms of the Doleans-Dade exponential (Protter 1990) as

$$E(J_t^i) \propto \exp(Y_t^i - 1/2[Y_t^i, Y_t^i]) \tag{3.16}$$

where $[Y_t^i, Y_t^i]$ is the quadratic variation of the stochastic process $Y_t^i$ (Protter 1990). Heuristically, by the Mean Value Theorem, if

$$1/2 d[Y_t^i, Y_t^i]/dt > dY_t^i/dt \tag{3.17}$$

then the pathological ground state is stable in expectation: deviations from nonequilibrium steady state measured by $E(J_t^i)$ converges to 0. That is, sufficient ongoing 'fog-of-war' noise—determining the quadratic variation terms in Eqs. (3.16) and (3.17)—can systematically lock-in system failure with high probability, in spite of managerial interventions to the contrary: hysteresis.

## 3.4 Groupoid Synergism Redux

Reiterating and sharpening a previous argument, it is possible to invoke something very similar to the symmetry breaking phase transition of Sect. 2.4, but in the context of the inherently cognitive nature of V2V/V2I systems. Traffic flow can be rephrased in terms of 'directed homotopy'—dihomotopy—groupoids on an underlying road network, again parameterized by the 'temperature' index $\mathscr{T}$. Classical homotopy characterizes topological structures in terms of the number of ways a loop within the object can be continuously reduced to a base point (Hatcher 2001). For a sphere, all loops can be reduced. For a toroid—a donut shape—there is a hole so that two classes of loops cannot be reduced to a point. One then composes loops to create the 'fundamental group' of the topological object. The construction is standard. Vehicles on a road network, however, are generally traveling from some initial point $So$ to a final destination $S1$, and directed paths, not loops are the 'natural' objects, at least over a short time period, as in commuting.

Given some 'hole' in the road network, there will usually be more than one way to reach $S1$ from $So$. An equivalence class of directed paths is defined by paths that can be deformed into one another without crossing barrier zones (Fajstrup et al. 2016; Grandis 2009). At high values of the composite index $\mathscr{T}$, many different sets of paths will be possible allowing unobstructed travel from one given point to another, defining equivalence classes creating a large groupoid. As $\mathscr{T}$ declines, roadways and junctions become increasingly jammed, eliminating entire equivalence classes of open pathways, and lowering the groupoid symmetry: phase transitions via classic symmetry breaking on a network. The 'order parameter' that disappears at high $\mathscr{T}$ is then simply the number of jammed roadways.

These results extend to higher dihomotopy groupoids via introduction of cylindrical paths rather than one-dimensional lines, producing a more general version of the quotient space geodesic method of Hu et al. (2001).

Most fundamentally, however, and as outlined earlier, the traffic flow groupoid and the groupoid associated with cognition across the V2V/V2I system will inevitably be intimately intertwined, synergistically compounding symmetry breaking traffic jams as-we-know-them with symmetry breaking cognitive collapse of the control system automata, creating conditions of monumental chaos.

# Chapter 4
# Conclusions

Ruelle (1983), in his elegant keynote address on turbulent dynamics, raises a red flag for any traffic flow studies:

> ...[A] deductive theory of developed turbulence does not exist, and a mathematical basis for the important theoretical literature on the subject is still lacking... A purely deductive analysis starting with the Navier-Stokes equation... does not appear feasible... and might be inappropriate because of the approximate nature of the... equation.

Or, as the mathematician Garrett Birkoff (1960, p.5) put it,

> ...[V]ery few of the deductions of rational hydrodynamics can be established rigorously.

Similar problems afflict the exactly solvable but highly approximate Black-Scholes models of financial engineering, and institutions that rely heavily on them have gone bankrupt in the face of market turbulence (Wallace 2015c).

Turbulence in traffic flow does not represent simple drift from steady linear or even parallel travel trajectories. Traffic turbulence involves the exponential amplification of small perturbations into large-scale deviations from complicated streamline geodesics in a topologically complex map quotient space. This is the mechanism of groupoid 'symmetry breaking' by which the system undergoes a phase transition from 'liquid' geodesic flow to 'crystalline' phases of shock fronts, platoons, and outright jams.

Under such circumstances, cognitive system initiative serves as a mechanism for returning to geodesic flows. Inhibition of cognitive initiative occurs when the composite density index $\Gamma$ exceeds a critical limit, triggering complex dynamic condensation patterns and, for autonomous vehicle systems, perhaps even more disruptive behaviors.

It is, then, not enough to envision atomistic autonomous ground vehicles as having only local dynamics in an embedding traffic stream, as seems the current American and European practice. Traffic light strategies, road quality, the usually rapid-shifting road map space, the dynamic composition of the traffic stream, bandwidth limits, and



R. Wallace, *Canonical Instabilities of Autonomous Vehicle Systems*,
SpringerBriefs in Computational Intelligence,
https://doi.org/10.1007/978-3-319-69935-6_4

so on, create the synergistic context in which single vehicles operate and which constitutes the individual 'driving experience'. It is necessary to understand the dynamics of that full system, not simply the behavior of a vehicle atom within it. The properties of that system will be both overtly and subtly emergent, as will, we assert, the responses of cognitive vehicles enmeshed in context, whether controlled by humans or computers.

One inference from this analysis is that failure modes afflicting large-scale V2V/V2I systems are likely to be more akin to power blackouts than to traffic jams as we know them, and the description by Kinney et al. (2005) is of interest:

> Today the North American power grid is one of the most complex and interconnected systems of our time, and about one half of all domestic generation is sold over ever-increasing distances on the wholesale market before it is delivered to customers... Unfortunately the same capabilities that allow power to be transferred over hundreds of miles also enable the propagation of local failures into grid-wide events... It is increasingly recognized that understanding the complex emergent behaviors of the power grid can only be understood from a systems perspective, taking advantage of the recent advances in complex network theory...

Dobson (2007) puts it as follows:

> [P]robabalistic models of cascading failure and power system simulations suggest that there is a critical loading at which expected blackout size sharply increases and there is a power law in the distribution of blackout size... There are two attributes of the critical loading: 1. A sharp change in gradient of some quantity such as expected blackout size as one passes through the critical loading. 2. A power law region in probability distribution of blackout size at the critical loading. We use the terminology 'critical' because this behavior is analogous to a critical phase transition in statistical physics.

Daqing et al. (2014), in fact, explicitly link traffic jams and power failures:

> Cascading failures have become major threats to network robustness due to their potential catastrophic consequences, where local perturbations can induce global propagation of failures... [that] propagate through collective interactions among system components.... [W]e find by analyzing our collected data that jams in city traffic and faults in power grid are spatially long-range correlated with correlations decaying slowly with distance. Moreover, we find in the daily traffic, that the correlation length increases dramatically and reaches maximum, when morning or evening rush hour is approaching...

While clever V2V/V2I management strategies might keep traffic streams in supercooled high-flow mode beyond critical densities, such a state is notoriously unstable, subject to both random and deliberately caused 'condensation' into large-scale frozen zones. More subtle patterns of autonomous vehicle 'psychopathology' may be even less benign, as studied in detail elsewhere (Wallace 2017).

'Blackout' considerations focus on macroscale phenomena. An example at an intermediate mesoscale involves 'platoon instabilities'.

To paraphrase di Bernado et al. (2015), 'platooning' describes the coordinated motion of groups of vehicles cooperating with each other to reach the same destination with a common velocity, usually envisioned as a close linear array so as to minimize overall air resistance, resulting in significantly improved fuel efficiency. Typical strategies focus on pairwise interactions based on local measurements by

onboard sensors: each vehicle only uses proximity information from its preceding agent in the platoon. The essential question for such a strategy involves 'string stability' in which perturbations affecting the leading vehicle are not amplified on down the line. The image is of the cracking of a whip. However, it has long been understood that simple pairwise interactions between vehicles can actually make long strings sensitive to such perturbations (e.g., Middleton and Braslavsly 2010). As di Bernardo et al. put it,

> Hence, there is a need to explore the use of more generic communication structures among vehicles... achieved through wireless [V2V] and [V2I] communication. The reference behavior is dispatched to all vehicles in the network by a leader vehicle belonging to the platoon (typically the first vehicle in the group). New challenges arise due to uncertainties and time-varying communication delays.

Such systems are characterized as operating under 'cooperative adaptive cruise control'—CACC.

CACC vehicle platooning thus comes very much under the draconian constrictions of the Data Rate Theorem: simple pairwise data exchange is inherently unstable and must be expanded to include information from each vehicle in the platoon, according to a complex topological protocol in which 'nodes' are vehicles characterized by their own dynamics, 'edges' model communication links between vehicles, and the structure of intervehicle communication is encoded in network topology. Ensuring string stability for such topologies is not trivial, and clearly must involve massive increase in available bandwidth over simple pairwise data exchange.

Interference with data exchange—bandwidth availability—or a rising need for bandwidth consequent on increasing $\rho$ or the composite $\Gamma$ of Sects. 2.1 and 2.2—will cause sudden, unexpected, and highly punctuated failure of coordinated platoon topology, with likely catastrophic outcomes for dangerous or valuable cargoes. Indeed, analogous problems have been studied by Amoozadeh et al. (2015), who examine security attacks on the communication channel as well as sensor tampering of a connected vehicle stream equipped to achieve CACC, finding that an insider attack can cause significant instability. Our results, however, suggest that the sudden onset of instabilities will likely be triggered by far more mundane factors such as bandwidth constrictions caused by signal overcrowding or high levels of random noise, perhaps as simple as nearby lightning strikes or sudden solar storm fluctuations.

For optical systems—LIDAR and cameras—fog, dust, rain or snow, sun glare, bright lights, a puff of exhaust or other smoke, will provide 'bandwidth' constraints contributing to an increase in $\Gamma$ and hence decline in the critical fog-of-war 'temperature' parameter $\mathscr{T}$.

Zhao et al. (2014) adapt the information theoretic methods of Martins et al. (2007) to study disturbance propagation in leader-follower systems with limited leader information—a specific form of CACC. Their 'Lemma 3', a key step in proving their central results is, as they note, closely reminiscent of the Data Rate Theorem.

Almost in passing, however, they comment

> As the literature on networked control systems demonstrates, even centralized control when information available to the controller is transmitted across communication channels displays a rich and non-obvious behavior. Although there has been some recent work on stabilizability of distributed systems... performance guarantees in distributed systems remain hard to obtain.

*Rich and non-obvious behavior.*

*Performance guarantees in distributed systems remain hard to obtain.*

It is difficult to escape the inference that, despite massive marketing hype and other wishful thinking, V2V/V2I autonomous vehicle systems may not be generally practical, particularly in a context of coupled social and infrastructure deterioration.

It has been said that 'The language of business is the language of dreams'. 'Business dreams', however, as we are now painfully learning at the national level, do not necessarily serve as a sound foundation for the design and implementation of public policies affecting the well-being of large populations.

# Chapter 5
# Mathematical Appendix

## 5.1 An RDT Approach to the DRT

The RDT asks how much a signal can be compressed and have average distortion, according to an appropriate measure, less than some predetermined limit $D$. The result is an expression for the minimum necessary channel capacity, $R$, as a function of $D$. See Cover and Thomas (2006) for details. Different channels have different expressions. For the Gaussian channel under the squared distortion measure,

$$R(D) = \frac{1}{2}\log[\frac{\sigma^2}{D}] \; D < \sigma^2$$
$$R(D) = 0 \; D \geq \sigma^2 \tag{5.1}$$

where $\sigma^2$ is the variance of channel noise having zero mean.

As above, we ask how a control signal $u_t$ is expressed in the system response $x_{t+1}$. We suppose it possible to deterministically retranslate an observed sequence of system outputs $x_1, x_2, x_3, ...$ into a sequence of possible control signals $\hat{u}_0, \hat{u}_1, ...$ and to compare that sequence with the original control sequence $u_0, u_1, ...$, with the difference between them having a particular value under the chosen distortion measure, and hence an observed average distortion.

The correspondence expansion is as follows.

Feynman (2000), expanding on ideas of Bennett, identifies information as a form of free energy. Thus $R(D)$, the minimum channel capacity necessary for average distortion $D$, is also a free energy measure, and we may define an entropy $S$ as

$$S \equiv R(D) - DdR/dD \tag{5.2}$$

For a Gaussian channel under the squared distortion measure,

$$S = 1/2\log[\sigma^2/D] + 1/2 \tag{5.3}$$

Other channels will have different expressions.



R. Wallace, *Canonical Instabilities of Autonomous Vehicle Systems*,
SpringerBriefs in Computational Intelligence,
https://doi.org/10.1007/978-3-319-69935-6_5

The simplest dynamics of such a system are given by a nonequilibrium Onsager equation in the gradient of $S$, (de Groot and Mazur 1984) so that

$$dD/dt = -\mu dS/dD = \frac{\mu}{2D} \tag{5.4}$$

By inspection,

$$D(t) = \sqrt{\mu t} \tag{5.5}$$

which is the classic outcome of the diffusion equation. For the 'natural' channel having $R(D) \propto 1/D$, $D(t) \propto$ the cube root of $t$.

This correspondence reduction allows an expansion to more complicated systems, in particular, to the control system of Fig. 2.1.

Let $\mathscr{H}$ be the rate at which control information is fed into an inherently unstable control system, in the presence of a further source of control system noise $\beta$, in addition to the channel noise defined by $\sigma^2$. The simplest generalization of Eq. (5.4), for a Gaussian channel, is the stochastic differential equation

$$dD_t = [\frac{\mu}{2D_t} - G(\mathscr{H})]dt + \beta D_t dW_t \tag{5.6}$$

where $dW_t$ represents white noise and $G(\mathscr{H}) \geq 0$ is a monotonically increasing function.

This equation has the nonequilibrium steady state expectation

$$D_{nss} = \frac{\mu}{2G(\mathscr{H})} \tag{5.7}$$

measuring the average distortion between what the control system wants and what it gets. In a sense, this is a kind of converse to the famous radar equation which states that a returned signal will be proportional to the inverse fourth power of the distance between the transmitter and the target. But there is an even deeper result to be found.

Applying the Ito chain rule to Eq. (5.6) (Protter 1990; Khashminskii 2012), it is possible to calculate the expected variance in the distortion as $E(D_t^2) - (E(D_t))^2$. But application of the Ito rule to $D_t^2$ shows that *no real number solution for its expectation is possible unless the discriminant of the resulting quadratic equation is* $\geq 0$, so that a necessary condition for stability is

$$\begin{aligned} G(\mathscr{H}) &\geq \beta\sqrt{\mu} \\ \mathscr{H} &\geq G^{-1}(\beta\sqrt{\mu}) \end{aligned} \tag{5.8}$$

where the second expression follows from the monotonicity of $G$.

As a consequence of the correspondence reduction leading to Eq. (5.5), we have generalized the DRT of Eq. (2.2). Different 'control channels', with different forms of $R(D)$, will give different detailed expressions for the rate of generation of 'topological information' by an inherently unstable system.

## 5.2 A Black-Scholes Model

Take $\mathscr{H}(\rho)$ as the control information rate 'cost' of stability at the level of crowding $\rho$. What is the mathematical form of $\mathscr{H}(\rho)$ under conditions of volatility i.e., variability in $\rho$ proportional to it? Let

$$d\rho_t = g(t, \rho_t)dt + b\rho_t dW_t \tag{5.9}$$

where $dW_t$ is taken as white noise and the function $g(t, \rho)$ will 'fall out' of the calculation on the assumption of certain regularities.

Let $\mathscr{H}(\rho_t, t)$ be the minimum needed incoming rate of control information under the Data Rate Theorem, and expand in $\rho$ using the Ito chain rule (Protter 1990)

$$\begin{aligned} d\mathscr{H}_t = [\partial\mathscr{H}/\partial t + g(\rho_t, t)\partial\mathscr{H}/\partial\rho + \frac{1}{2}b^2\rho_t^2\partial^2\mathscr{H}/\partial\rho^2]dt \\ +[b\rho_t\partial\mathscr{H}/\partial\rho]dW_t \end{aligned} \tag{5.10}$$

Define a quantity $L$ as a Legendre transform of the rate $\mathscr{H}$ by convention having the form

$$L = -\mathscr{H} + \rho\partial\mathscr{H}/\partial\rho \tag{5.11}$$

Since $\mathscr{H}$ is an information index, it is a kind of free energy in the sense of Feynman (2000) and $L$ is a classic entropy measure.

Heuristically, replacing $dX$ with $\Delta X$ in these expressions and applying Eq. (5.10),

$$\Delta L = (-\partial\mathscr{H}/\partial t - \frac{1}{2}b^2\rho^2\partial^2\mathscr{H}/\partial\rho^2)\Delta t \tag{5.12}$$

As in the classical Black-Scholes model (Black and Scholes 1973), the terms in $g$ and $dW_t$ 'cancel out', and the effects of noise are subsumed into the Ito correction factor, a regularity assumption making this an exactly solvable but highly approximate model.

The conventional Black-Scholes calculation takes $\Delta L/\Delta T \propto L$. Here, at non-equilibrium steady state, we assume $\Delta L/\Delta t = \partial\mathscr{H}/\partial t = 0$, so that

$$-\frac{1}{2}b^2\rho^2\partial^2\mathscr{H}/\partial\rho^2 = 0 \tag{5.13}$$

By inspection,

$$\mathscr{H} = \kappa_1\rho + \kappa_2 \tag{5.14}$$

where the $\kappa_i$ are nonnegative constants.

## 5.3 Groupoids

Given a pairing, for example connection by a meaningful path to the same basepoint, it is possible to define 'natural' end-point maps $\alpha(g) = a_j, \beta(g) = a_k$ from the set of morphisms $G$ into $A$, and a formally associative product in the groupoid $g_1 g_2$ provided $\alpha(g_1 g_2) = \alpha(g_1), \beta(g_1 g_2) = \beta(g_2)$, and $\beta(g_1) = \alpha(g_2)$. Then the product is defined, and associative, i.e., $(g_1 g_2) g_3 = g_1 (g_2 g_3)$, with inverse defined by $g = (a_j, a_k), g^{-1} \equiv (a_k, a_j)$.

In addition there are natural left and right identity elements $\lambda_g, \rho_g$ such that $\lambda_g g = g = g \rho_g$.

An orbit of the groupoid $G$ over $A$ is an equivalence class for the relation $a_j \sim G a_k$ if and only if there is a groupoid element $g$ with $\alpha(g) = a_j$ and $\beta(g) = a_k$. Following Cannas Da Silva and Weinstein (1999), a groupoid is called transitive if it has just one orbit. The transitive groupoids are the building blocks of groupoids in that there is a natural decomposition of the base space of a general groupoid into orbits. Over each orbit there is a transitive groupoid, and the disjoint union of these transitive groupoids is the original groupoid. Conversely, the disjoint union of groupoids is itself a groupoid.

The isotropy group of $a \in X$ consists of those $g$ in $G$ with $\alpha(g) = a = \beta(g)$. These groups prove fundamental to classifying groupoids.

If $G$ is any groupoid over $A$, the map $(\alpha, \beta) : G \to A \times A$ is a morphism from $G$ to the pair groupoid of $A$. The image of $(\alpha, \beta)$ is the orbit equivalence relation $\sim G$, and the functional kernel is the union of the isotropy groups. If $f : X \to Y$ is a function, then the kernel of $f$, $ker(f) = [(x_1, x_2) \in X \times X : f(x_1) = f(x_2)]$ defines an equivalence relation.

Groupoids may have additional structure. As Weinstein (1996) explains, a groupoid $G$ is a topological groupoid over a base space $X$ if $G$ and $X$ are topological spaces and $\alpha, \beta$ and multiplication are continuous maps. A criticism sometimes applied to groupoid theory is that their classification up to isomorphism is nothing other than the classification of equivalence relations via the orbit equivalence relation and groups via the isotropy groups. The imposition of a compatible topological structure produces a nontrivial interaction between the two structures. Below we will introduce a metric structure on manifolds of related information sources, producing such interaction.

In essence a groupoid is a category in which all morphisms have an inverse, here defined in terms of connection by a meaningful path of an information source dual to a cognitive process.

As Weinstein (1996) points out, the morphism $(\alpha, \beta)$ suggests another way of looking at groupoids. A groupoid over $A$ identifies not only which elements of $A$ are equivalent to one another (isomorphic), but *it also parameterizes the different ways (isomorphisms) in which two elements can be equivalent*, i.e., all possible information sources dual to some cognitive process. Given the information theoretic characterization of cognition presented above, this produces a full modular cognitive network in a highly natural manner.

Brown (1987) describes the basic structure as follows:

> A groupoid should be thought of as a group with many objects, or with many identities... A groupoid with one object is essentially just a group. So the notion of groupoid is an extension of that of groups. It gives an additional convenience, flexibility and range of applications...
>
> EXAMPLE 1. A disjoint union [of groups] $G = \cup_\lambda G_\lambda, \lambda \in \Lambda$, is a groupoid: the product $ab$ is defined if and only if $a, b$ belong to the same $G_\lambda$, and $ab$ is then just the product in the group $G_\lambda$. There is an identity $1_\lambda$ for each $\lambda \in \Lambda$. The maps $\alpha, \beta$ coincide and map $G_\lambda$ to $\lambda, \lambda \in \Lambda$.
>
> EXAMPLE 2. An equivalence relation $R$ on [a set] $X$ becomes a groupoid with $\alpha$, $\beta : R \to X$ the two projections, and product $(x, y)(y, z) = (x, z)$ whenever $(x, y), (y, z) \in R$. There is an identity, namely $(x, x)$, for each $x \in X$...

Weinstein (1996) makes the following fundamental point:

> Almost every interesting equivalence relation on a space $B$ arises in a natural way as the orbit equivalence relation of some groupoid $G$ over $B$. Instead of dealing directly with the orbit space $B/G$ as an object in the category $S_{map}$ of sets and mappings, one should consider instead the groupoid $G$ itself as an object in the category $G_{htp}$ of groupoids and homotopy classes of morphisms.

It is possible to explore homotopy in paths generated by information sources.

**Global and local groupoids**

The argument next follows Weinstein (1996) fairly closely, using his example of a finite tiling.

Consider a tiling of the euclidean plane $R^2$ by identical 2 by 1 rectangles, specified by the set $X$ (one dimensional) where the grout between tiles is $X = H \cup V$, having $H = R \times Z$ and $V = 2Z \times R$, where $R$ is the set of real numbers and $Z$ the integers. Call each connected component of $R^2 \backslash X$, i.e. the complement of the two dimensional real plane intersecting $X$, a tile.

Let $\Gamma$ be the group of those rigid motions of $R^2$ which leave $X$ invariant, i.e., the normal subgroup of translations by elements of the lattice $\Lambda = H \cap V = 2Z \times Z$ (corresponding to corner points of the tiles), together with reflections through each of the points $1/2\Lambda = Z \times 1/2Z$, and across the horizontal and vertical lines through those points. As noted in Weinstein (1996), much is lost in this coarse-graining, in particular the same symmetry group would arise if we replaced $X$ entirely by the lattice $\Lambda$ of corner points. $\Gamma$ retains no information about the local structure of the tiled plane. In the case of a real tiling, restricted to the finite set $B = [0, 2m] \times [0, n]$ the symmetry group shrinks drastically: The subgroup leaving $X \cap B$ invariant contains just four elements even though a repetitive pattern is clearly visible. A two-stage groupoid approach recovers the lost structure.

We define the transformation groupoid of the action of $\Gamma$ on $R^2$ to be the set

$$G(\Gamma, R^2) = \{(x, \gamma, y | x \in R^2, y \in R^2, \gamma \in \Gamma, x = \gamma y\}$$

with the partially defined binary operation

$$(x, \gamma, y)(y, \nu, z) = (x, \gamma\nu, z).$$

Here $\alpha(x, \gamma, y) = x$, and $\beta(x, \gamma, y) = y$, and the inverses are natural.
We can form the restriction of $G$ to $B$ (or any other subset of $R^2$) by defining

$$G(\Gamma, R^2)|_B = \{g \in G(\Gamma, R^2) | \alpha(g), \beta(g) \in B\}$$

1. An orbit of the groupoid $G$ over $B$ is an equivalence class for the relation $x \sim_G y$ if and only if there is a groupoid element $g$ with $\alpha(g) = x$ and $\beta(g) = y$. Two points are in the same orbit if they are similarly placed within their tiles or within the grout pattern.
2. The isotropy group of $x \in B$ consists of those $g$ in $G$ with $\alpha(g) = x = \beta(g)$. It is trivial for every point except those in $1/2\Lambda \cap B$, for which it is $Z_2 \times Z_2$, i.e. the direct product of integers modulo two with itself.

By contrast, embedding the tiled structure within a larger context permits definition of a much richer structure, i.e. the identification of local symmetries.

We construct a second groupoid as follows: Consider the plane $R^2$ as being decomposed as the disjoint union of $P_1 = B \cap X$ (the grout), $P_2 = B \backslash P_1$ (the complement of $P_1$ in $B$, i.e. the tiles), and $P_3 = R^2 \backslash B$ (the exterior of the tiled room). Let $E$ be the group of all euclidean motions of the plane, and define the local symmetry groupoid $G_{loc}$ as the set of triples $(x, \gamma, y)$ in $B \times E \times B$ for which $x = \gamma y$, and for which $y$ has a neighborhood $\mathscr{U}$ in $R^2$ such that $\gamma(\mathscr{U} \cap P_i) \subseteq P_i$ for $i = 1, 2, 3$. The composition is given by the same formula as for $G(\Gamma, R^2)$.

For this groupoid-in-context there are only a finite number of orbits:

$\mathscr{O}_1$ = interior points of the tiles.
$\mathscr{O}_2$ = interior edges of the tiles.
$\mathscr{O}_3$ = interior crossing points of the grout.
$\mathscr{O}_4$ = exterior boundary edge points of the tile grout.
$\mathscr{O}_5$ = boundary 'T' points.
$\mathscr{O}_6$ = boundary corner points.

The isotropy group structure is, however, now very rich indeed:

The isotropy group of a point in $\mathscr{O}_1$ is now isomorphic to the entire rotation group $O_2$.

It is $Z_2 \times Z_2$ for $\mathscr{O}_2$.

For $\mathscr{O}_3$ it is the eight-element dihedral group $D_4$.

For $\mathscr{O}_4$, $\mathscr{O}_5$ and $\mathscr{O}_6$ it is simply $Z_2$.

These are the 'local symmetries' of the tile-in-context.

## 5.4 Morse Theory

Morse theory examines relations between analytic behavior of a function—the location and character of its critical points—and the underlying topology of the manifold on which the function is defined. We are interested in a number of such functions, for example information source uncertainty on a parameter space and 'second order'

iterations involving parameter manifolds determining critical behavior, for example sudden onset of a giant component in a network model. We follow Pettini (2007).

The central argument of Morse theory is to examine an $n$-dimensional manifold $M$ as decomposed into level sets of some function $f : M \to \mathbf{R}$ where $\mathbf{R}$ is the set of real numbers. The $a$-level set of $f$ is defined as

$$f^{-1}(a) = \{x \in M : f(x) = a\},$$

the set of all points in $M$ with $f(x) = a$. If $M$ is compact, then the whole manifold can be decomposed into such slices in a canonical fashion between two limits, defined by the minimum and maximum of $f$ on $M$. Let the part of $M$ below $a$ be defined as

$$M_a = f^{-1}(-\infty, a] = \{x \in M : f(x) \leq a\}.$$

These sets describe the whole manifold as $a$ varies between the minimum and maximum of $f$.

Morse functions are defined as a particular set of smooth functions $f : M \to \mathbf{R}$ as follows. Suppose a function $f$ has a critical point $x_c$, so that the derivative $df(x_c) = 0$, with critical value $f(x_c)$. Then $f$ is a Morse function if its critical points are nondegenerate in the sense that the Hessian matrix $\mathscr{J}$ of second derivatives at $x_c$, whose elements, in terms of local coordinates are

$$\mathscr{J}_{i,j} = \partial^2 f / \partial x^i \partial x^j,$$

has rank $n$, which means that it has only nonzero eigenvalues, so that there are no lines or surfaces of critical points and, ultimately, critical points are isolated.

The index of the critical point is the number of negative eigenvalues of $\mathscr{J}$ at $x_c$.

A level set $f^{-1}(a)$ of $f$ is called a critical level if $a$ is a critical value of $f$, that is, if there is at least one critical point $x_c \in f^{-1}(a)$.

Again following Pettini (2007), the essential results of Morse theory are as follows:

1. If an interval $[a, b]$ contains no critical values of $f$, then the topology of $f^{-1}[a, v]$ does not change for any $v \in (a, b]$. Importantly, the result is valid even if $f$ is not a Morse function, but only a smooth function.
2. If the interval $[a, b]$ contains critical values, the topology of $f^{-1}[a, v]$ changes in a manner determined by the properties of the matrix $\mathscr{J}$ at the critical points.
3. If $f : M \to \mathbf{R}$ is a Morse function, the set of all the critical points of $f$ is a discrete subset of $M$, i.e., critical points are isolated. This is Sard's Theorem.
4. If $f : M \to \mathbf{R}$ is a Morse function, with $M$ compact, then on a finite interval $[a, b] \subset \mathbf{R}$, there is only a finite number of critical points $p$ of $f$ such that $f(p) \in [a, b]$. The set of critical values of $f$ is a discrete set of $\mathbf{R}$.
5. For any differentiable manifold $M$, the set of Morse functions on $M$ is an open dense set in the set of real functions of $M$ of differentiability class $r$ for $0 \leq r \leq \infty$.
6. Some topological invariants of $M$, that is, quantities that are the same for all the manifolds that have the same topology as $M$, can be estimated and sometimes computed exactly once all the critical points of $f$ are known: let the Morse numbers

$\mu_i (i = 0, ..., m)$ of a function $f$ on $M$ be the number of critical points of $f$ of index $i$, (the number of negative eigenvalues of $H$). The Euler characteristic of the complicated manifold $M$ can be expressed as the alternating sum of the Morse numbers of any Morse function on $M$,

$$\chi = \sum_{i=1}^{m} (-1)^i \mu_i .$$

The Euler characteristic reduces, in the case of a simple polyhedron, to

$$\chi = V - E + F$$

where $V$, $E$, and $F$ are the numbers of vertices, edges, and faces in the polyhedron.

7. Another important theorem states that, if the interval $[a, b]$ contains a critical value of $f$ with a single critical point $x_c$, then the topology of the set $M_b$ defined above differs from that of $M_a$ in a way which is determined by the index, $i$, of the critical point. Then $M_b$ is homeomorphic to the manifold obtained from attaching to $M_a$ an $i$-handle, i.e., the direct product of an $i$-disk and an $(m-i)$-disk.

Matsumoto (2002) and Pettini (2007) provide details and further references.

# Chapter 6
# References


Amoozadeh M, Raghuramu A, Dhuah C, Ghosal D, Xhang HMZ, Rowe J, Levitt K (2015) Security vulnerabilites of connected vehicle streams and their impact on cooperative driving. IEEE Commun Mag 53:126–132

Appleby J, Mao X, Rodkina A (2008) Stabilization and destabilization of nonlinear differential equations by noise. IEEE Trans Autom Control 53:683–691

Birkoff G (1960) Hydrodynamics: a study in logic, fact, and similitude, 2nd edn. Princeton University Press, Princeton, NJ

Black F, Scholes M (1973) The pricing of options and corporate liabilities. J Popul Econ 81:637–654

Blandin S et al (2011) A general phase transition model for vehicular traffic. SIAM J Appl Math 71:107–127

Bottcher L, Nagler J, Hermann H (2017) Critical behaviors in contagion dynamics. Phys Rev Lett 118:088301

Box G, Draper N (1987) Empirical Model-Building and response surfaces. Wiley, New York

Cassidy M, Jang K, Daganzo C (2011) Macroscopic fundamental diagrams for freeway networks. Trans Res Rec 2260:8–15

Corless R, Gonnet G, Hare D, Jeffrey D, Knuth D (1996) On the Lambert W function. Adv Comp Math 4:329–359

Daqing L, Yinan J, Rui K, Havlin S (2014) Spatial correlation analysis of cascading failures: congestions and blackouts. Sci Rep 4:5381

de Groot S, Mazur P (1984) Nonequilibrium thermodynamics. Dover, New York

di Bernardo M, Salvi A, Santini S (2015) Distributed consensus strategy for platooning of vehicles in the presence of time-varying heterogeneous communication delays. IEEE Trans Intell Transp Syst 16:102–112

Dobson I (2007) Where is the edge for cascading failure?: challenges and opportunities for quantifying blackout risk. IEEE Power Engineering Society General Meeting, Tampa Fl. USA (dobson@engr.wisc.edu)

Dzganzo C, Gayah V, Gonzales E (2010) Macroscopic relations of urban traffic variables: an analysis of instability. Working Paper UCB-ITS-VWP-2010-4, UC Berkeley Center for Future Urban Transit

Fajstrup L, Goubault E, Mourgues A, Mimram S, Raussen M (2016) Directed algebraic topology and concurrency. Springer, New York

Geroliminis N, Daganzo C (2008) Existence of urban-scale macroscopit fundamental diagrams: some experimental findings. Trans Res B 42:759–770




R. Wallace, *Canonical Instabilities of Autonomous Vehicle Systems*,
SpringerBriefs in Computational Intelligence,
https://doi.org/10.1007/978-3-319-69935-6_6

Geroliminis N, Sun J (2011a) Properties of a well-defined macroscopic fundamental diagram for urban traffic Trans Res B 45:605–617
Geroliminis N, Sun J (2011b) Hysteresis phenomena of a macroscopic fundamental diagram in freeway networks. Trans Res B 45:966–979
Glazebrook JF, Wallace R (2009) Rate distortion manifolds as model spaces for cognitive information. Informatica 33:309–345
Gould P, Wallace R (1994) Spatial structures and scientific paradox in the AIDS epidemic. Geogr Ann 76B:105–116
Grandis M (2009) Directed algebraic topology: models of Non-Reversible worlds. Cambridge University Press, New York
Hatcher A (2001) Algebraic topology. Cambridge University Press, New York
Helbing D (2001) Traffic and related self-driven many-particle systems. Rev Mod Phys 73:1067–1141
Hu J, Prandini M, Johnasson K, Sastry S (2001) Hybrid geodesics as optimal solutions to the collision-free motion planning problem. In: Di Benedetto M, Sangiovanni-Vincentelli A (eds) HSCC 2001, LNCS 2034:305–318
Jin C et al (2013) Spontaneous phase transition from free flow to synchronized flow in traffic on a single-lane highway. Phys Rev E 87:012815
Kerner B, Klenov S (2009) Phase transitions in traffic flow on multilane roads. Phys Rev E 80:056101
Kerner B, Koller M, Klenov S, Rehborn H, Leibel M (2015) Empirical features of spontaneous and induced traffic breakdowns in free flow at highway bottlenecks. arXiv:1502.02862v2 [physics.soc-ph]
Khasminskii R (2012) Stochastic stability of differential equations, 2nd edn. Springer, New York
Kinney R et al (2005) Modeling cascading failures in the North American power grid. Eur Phys J B 46:101–107
Landau L, Lifshitz E (1987) Fluid mechanics, 2nd edn. Pergamon Press, NY
Li D, Fu B, Wang Y, Lu G, Berezin Y, Stanley HE (2015) Percolation transition in dynamical traffic network with evolving critical bottlenecks. PNAS 112:669–672
Luczak T (1990) Component behavior near the critical point of the random graph process, Random Struct Algo 1:287–310
Maerivoet S, De Moor B (2006) Data quality travel time estimation and reliability. Katholieke University Leuven 06–030
Mao X (1996) Stochastic self-stabilization. Stochast Stochast Rep 57:57–70
Mao X (2007) Stochastic differential equations and applications, 2nd edn. Woodhead Publishing, Philadelphia
Martins N, Dahleh M, Doyle J (2007) Fundamentel limitations of disturbance attenuation in the presence of side information. IEEE Trans Autom Control 52:56–66
Matsumoto Y (2002) An introduction to morse theory. American Mathematical Society, Providence RI
Middleton R, Braslavsky J (2010) String instability in classes of linear time invariant formation control with limited communication range. IEEE Trans Autom Control 55:1519–1530
Molloy M, Reed B (1995) A critical point for random graphs with a given degree sequence. Rand Str Algor 6:161–179
Molloy M, Reed B (1998) The size of the giant component of a random graph with a given degree sequence. Comb Probab Comput 7:295–305
Nair G, Fagnani F, Zampieri S, Evans R (2007) Feedback control under data rate constraints: an overview. Proc IEEE 95:108–137
Newman M, Strogatz S, Watts D (2001) Random graphs with arbitrary degree distributions and their applications. Phys Rev E 64(026118):1–17
Ohira T, Sawatari R (1998) Phase transition in a computer network traffic model. Phys Rev E 58:193–195
Orosz G, Wilaon RE, Stepan G (2010) Traffic jams: dynamics and control. Phil Trans R Soc A 368:4455–4479

Pettini M (2007) Geometry and topology in Hamiltonian systems. Springer, New York
Protter P (1990) Stochastic integration and differential equations. Springer, New York
Ramaswamy S (2010) The mechanics and statistics of active matter. Ann Rev Condens Matter Phys 1:323–345
The Rand Fire Project (1979) Fire deployment analysis: a public policy analysis case study. North Holland, New York
Ruelle D (1983) Turbulent dynamical systems, Proceedings of the International Congress of Mathematicians, Warsaw, pp 271–286, 16–24 Aug 1983
Sole R, Valverde S (2001) Information transfer and phase transition in a model of internet traffic. Phys A 289:595–605
Sugiyama Y, Fukui M, Kikuchi M, Hasebe K, Nakayama A, Nishinari K, Tadaki S, Yukawa S (2008) Traffic jams without bottlenecks–experimental evidence for the physical mechanism fo the formation of a jam. New J Phys 10:033001
Wallace D, Wallace R (1998) A plague on your houses. Verso, New York
Wallace R, Wallace D (2013) A mathematical approach to multilevel, multiscale health interventions: pharmaceutical industry decline and policy response. Imperial College Press, London
Wallace R (2012) Consciousness, crosstalk, and the mereological fallacy: an evolutionary perspective. Phys Life Rev 9:426–453
Wallace R (2014) Extending swerdlow's hypothesis: statistical models of mitochondrial deterioration and aging. J Math Chem 52:2663–2679
Wallace R (2015a) Closed-system 'economic' models for psychiatric disorders: western atomism and its culture-bound syndromes. Cogn Process 16:279–290
Wallace R (2015b) An information approach to mitochondrial dysfunction. World Scientific, Singapore
Wallace R (2015c) An ecosystem approach to economic stabilization: escaping the neoliberal wilderness. Routledge Advances in Heterodox Economics, London
Wallace R (2016a) Subtle noise structures as control signals in high-order biocognition. Phys Lett A https://doi.org/10.1016/j.physleta.2015.11.037
Wallace R (2017) Information theory models of instabilities in critical systems. World Scientific, Singapore
Weinstein A (1996) Groupoids: unifying internal and external symmetry. Not Am Math Soc 43:744–752
Zhang L (2015) Realistic, efficient and secure geographic routing in vehicular networks. PhD thesis, Department of Computer Science, University of Victoria, Canada
Zhao Y, Minero P, Gupta V (2014) On disturbance propagation in leader-follower systems with limited leader information. Automatica 50:591–598